

https://dspace.org/

An Assessment of Hyperostosis Frontalis Interna Within a South African Skeletal Sample

Moraba, Mmanoko Irene

2025
University of the Witwatersrand, Johannesburg
https://hdl.handle.net/10539/49840

Moraba, Mmanoko Irene . (2025). An Assessment of Hyperostosis Frontalis Interna Within a South African Skeletal Sample [Master's dissertation, University of the Witwatersrand, Johannesburg]. WIReDSpace. https://hdl.handle.net/10539/49840

Downloaded from a DSpace repository. https://dspace.org/

AN ASSESSMENT OF HYPEROSTOSIS FRONTALIS INTERNA WITHIN A SOUTH AFRICAN SKELETAL SAMPLE



Name: Mmanoko Irene Moraba

Student Number: 1702036

Supervisors: Dr. A. Meyer

Prof. E.F. Hutchinson

Master of Science (Medicine)

Department of Anatomical Sciences

School of Biomedical Sciences

Table of Contents

List of tables 5

List of figures 7

PLAGIARISM DECLARATION 9

ACKNOWLEDGEMENTS 10

ABSTRACT 11

1. INTRODUCTION 12

2. LITERATURE REVIEW 14

2.1. Prevalence of HFI in archaeological and modern population 14

2.2. Sex and age distribution of HFI 15

2.3. Aetiology of HFI 16

2.4. Pathogenesis of HFI 19

2.5. Diagnostic Imaging Technique 20

3. AIMS AND OBJECTIVES 23

4. MATERIALS AND METHODS 23

4.1. Study sample 24

4.2. Morphological scoring criteria 29

4.3. Micro-architectural criteria 30

4.4. Micro-architectural parameters 33

4.5. Statistical analysis 33

4.5.1. Morphological scoring method 33

4.5.2. Micro-architecture 34

5. RESULTS 35

5.1. HFI expression in the sample 35

5.2. Intra- and inter-observer reliability 41

5.3. Distribution of HFI according to sex and population affinity 41

5.3.1. Distribution of HFI according to age 44

5.4. Intra- and inter-observer reliability for the microarchitectural parameters 46

5.5. Micro-architectural differences between individuals with and without HFI 47

5.5.1. Sex differences in HFI and control group 50

5.5.2. Population differences in HFI and control groups 56

5.5.3. Age correlation 60

5.6. Severity of HFI 63

6. DISCUSSION 68

7. CONCLUSION 82

REFERENCES 84

Appendix A. Ethics waiver from the Human Ethics Research Committee of the University of the Witwatersrand permitting for the use of skeletal samples from Raymond A. Dart collection. 91

Appendix B: An assessment of age normality within HFI types using the Shapiro–Wilk Test. 92

Appendix C: An assessment of normality in HFI type distribution among population groups using the Shapiro–Wilk Test. 94

Appendix D: An assessment of normality in HFI type distribution among sexes using the Shapiro–Wilk Test. 94

Appendix E. Shapiro–wilk test of normality for Micro-CT variables assessed in control (C) and HFI groups. 94

D, density; BS/BV, bone surface to bone volume; BV/TV, bone volume to tissue volume; TBN, trabecular number; TBSP, trabecular spacing; and TBTH, trabecular thickness.

Region A, Measurements across the infraorbital region and region B, measurements across the lateral nasal aperture. A1/B1 denotes extracranial, B1/B2 middle, and B3/B3 endocranial surfaces 96

Appendix F. Distribution of individuals assessed with absence of HFI (*n* = 1811)..... 96

Appendix G: Distribution of HFI types in females, by age and population groups. 97

Appendix H: Distribution of HFI types in males, by age and population groups. 98

List of tables

Table 1. Individuals assessed (n = 2186) and individuals presenting with HFI (n = 375) in the Raymond A. Dart Collection of Human Skeletons were sorted by population affinity, age, and sex. 25
Table 2. Micro-architectural sample (n = 30) representing age-at-death categories (10-year cohorts) for adult individuals in the Raymond A. Dart Collection of Modern Human Skeletons by population affinity and sex..... 28
Table 3. An overview of intra- and inter-observer repeatability results using Lin's concordance correlation coefficient (Lin's CCC), with the estimated CCC values and their corresponding 95% confidence intervals (CI)..... 47
Table 4. Micro-architectural parameters in individuals with and without HFI (SD - standard deviation) across the infraorbital foramen region. 49
Table 5. Micro-architectural parameters in individuals with and without HFI (SD - standard deviation) across the lateral nasal aperture region. 50
Table 6. Micro-architectural parameters in males with and without HFI (SD - standard deviation) across the infraorbital foramen region. 51
Table 7. Micro-architectural parameters in males with and without HFI (SD - standard deviation) across the lateral nasal aperture region. 53
Table 8. Micro-architectural parameters in females with and without HFI (SD - standard deviation) across the infraorbital foramen region. 54
Table 9. Micro-architectural parameters in females with and without HFI (SD - standard deviation) across the lateral nasal aperture region. 55
Table 10. Micro-architectural parameters differences in populations with and without HFI (SD - standard deviation) across the infraorbital foramen region. 57
Table 11. Micro-architectural parameters differences in populations with and without HFI (SD - standard deviation) across the lateral nasal aperture region. 59
Table 12. Overview of the correlation coefficients (r) between micro-architectural parameters and age across the infraorbital foramen region in HFI and control groups. 61
Table 13. Overview of the correlation coefficients (r) between micro-architectural parameters and age across the lateral nasal aperture in HFI and control groups. 63

Table 14. Micro-architectural parameters of cortical and trabecular bone for various HFI types across the infraorbital foramen region. 65
Table 15. Micro-architectural parameters of cortical and trabecular bone for various HFI types across the lateral nasal aperture region. 67

List of figures

Figure 1: Schematic presentation of HFI types A–D relative to the endocranial surface of the human frontal bone extracted from Hershkovitz *et al*. (1999), pp.307 (Fig. 1. Schematic presentation of HFI types A–D). 30
Figure 2. An anterior view of the cranium indicates the sagittal reference plane (red) established after selecting fiducial landmarks. Vertical lines (yellow) represent the sagittal planes aligned to the selected cranial sites of the frontal bone where regions of interest were selected. 32
Figure 3. Micro-CT scans showing sagittal sections through the cranium at: A. infraorbital foramen, B. lateral nasal aperture (i.e., regions of interest). A1/A3/B1/B3 represent the cortical bone and A2/B2 represent the trabecular bone. 32
Figure 4. Intracranial views of skulls presenting with HFI Type A showing an isolated, elevated bony island(s), single (A1) or multiple (A2), unilateral (A1) or bilateral (A2), all with discrete, often undermined margins (arrows). Image A1 represents a 61-year-old SA Black male, and A2 is a 45-year-old SA Black male. 36
Figure 5. Intracranial views of skulls presenting with HFI Type B show a bony overgrowth(s) without discrete margins (oval (B1)) and slight elevation (arrow (B2)). Occasionally, isolated nodular areas were also identified (circles). Image B1 represents a 46-year-old SA Coloured Female, and B2, a 63-year-old SA White female. 37
Figure 6. An intracranial view of the skull of a 48-year-old SA Black male presenting with HFI Type C showing the expansion of coalesced nodules and irregular thickening of the frontal bone (arrows). 39
Figure 7. An intracranial view of skulls presenting with HFI Type D is characterised by extensive thickening of the intracranial surface extending to the parietal and temporal bones (black arrows (D1)). Type D exhibits clustered lobulations or a cauliflower shape (D2). Image D1 represents an 85-year-old SA White female, and D2 in an 82-year-old SA White female. Mm (red arrow) represents the middle meningeal artery groove. 40
Figure 8. Distribution of females and males presenting with various types of HFI. 41
Figure 9. Distribution of South African Black, South African White and South African Coloured samples presenting with various types of HFI. 42

Figure 10. Distribution of individuals presenting with various types of HFI in different age cohorts i.e., 20-49 years (young age), 50-69 years (middle age) and 70+ years (old age)..... 44
Figure 11. A Scatter plot indicating the correlation between age and the severity of HFI..... 45
Figure 12. Micro-CT images of individuals presenting HFI Type A, B, C and D through the cranium at the infraorbital foramen region. The colour-coded line reflects variations in density levels. In this gradient, red signifies the highest density, followed by yellow, green, and blue, representing the lowest density..... 64

PLAGIARISM DECLARATION

I Mmanoko Irene Moraba declare that this Dissertation is my own, unaided work. It is being submitted for the Degree of Master of Science in Medicine (Dissertation) at the University of the Witwatersrand, Johannesburg. It has not been submitted before for any degree or examination at any other University.



(Signature of candidate)

25th day of August 2025 in Auckland Park

ACKNOWLEDGEMENTS

The following individuals and institutions have my sincere gratitude for their tremendous assistance, direction, and encouragement in helping me finish this dissertation:

To my supervisors, Dr. Anja Meyer and Prof. Erin Hutchinson, thank you for your invaluable guidance, patience, and constructive feedback throughout this academic journey.

I am grateful to Mr. Anteneh Yalew, the faculty Biostatistician, for his assistance with data analysis. Your patience and willingness to help are truly appreciated.

I am also thankful to Dr. Billings for encouraging me to continue with my research after receiving a job offer and thought of dropping out. Thank you for helping me believe that it is truly possible to balance both.

To my friends and family, thank you for your emotional support and for keeping me grounded.

I also would like to extend my gratitude to the National Research Foundation, the JJJ Smieszek Fellowship, and Wits SRC #PavingTheNext100 for their financial support.

“Last but not least, I want to thank me. I want to thank me for believing in me, I want to thank me for doing all this hard work, I want to thank me for having no days off, I want to thank me for never quitting.”- Snoop Dog

ABSTRACT

Hyperostosis frontalis interna (HFI) is a condition characterised by bony outgrowths located unilaterally or bilaterally on the intracranial surface of the anterior frontal bone. The prevalence and microarchitecture of this condition are poorly studied in South Africa. This study aimed to assess the prevalence, expression, and severity of HFI in a South African skeletal sample using a morphological approach and gain insight into the aetiology and pathogenesis of HFI by looking at the micro-architectural changes in affected cranial areas. A total of 2186 adult crania (20 - 90+ years) were sourced from the Raymond A. Dart Collection of Modern Human Skeletons to assess the prevalence and expression of HFI morphologically. HFI was observed in 17.15% (n = 375) of the cranial vaults assessed (n = 2186), with higher prevalence in females (n = 243/375, 64.8%) compared to males (n = 132/375, 35.2%), SA Black sample (n = 209/375; 55.73%) and middle-aged (50 - 69 years) individuals (n = 143/375; 38.13%). Intra-observer reliability for the morphological classification showed strong agreement (k = 0.891, $p < .001$), while inter-observer reliability was moderate (k = 0.713, $p < .001$). After the classification of HFI, 15 individuals with HFI and 15 without HFI were scanned using a Nikon XTH 225L Micro-CT X-ray unit to evaluate possible differences in the micro-architectural features of affected and unaffected crania at predetermined regions of interest. Poor agreement was observed for most intra- and inter-observer measurements of microarchitecture (CCC = -0.05 to 0.59), except for trabecular spacing (TbSp), which showed perfect intra-observer agreement (CCC = 1.00). An increased bone mineral density and bone-surface-bone-volume ratio were observed in individuals with HFI in both cortical and trabecular regions. Males with HFI displayed a significant decrease in the bone-volume-to-tissue-volume ratio, particularly in the endocranial cortical bone at the infraorbital foramen, while females with HFI exhibited decreased bone mineral density (BMD) in both the cortical and trabecular regions and decreased trabecular number (TBN) compared to females without HFI. Hershkovitz *et al*. (1999) scoring criteria can be effectively used to score HFI; however, modifications to the Type D classification are recommended to account for cases where HFI extends beyond the frontal bone. The prevalence and degree of HFI vary within populations, between sexes, and between age groups, highlighting the importance of demographic factors when studying the prevalence and aetiology of HFI. Based on microarchitectural results, we can

conclude that the microarchitectural structure of the frontal bone varies between individuals with and without HFI, across sex, age, and population affinity groups.

Keywords: Ordinal scoring, Palaeopathology, Micro-computed tomography, Bone morphology, Bone microarchitecture

1. INTRODUCTION

Rapid urbanisation reshaped the demographic characteristics of human populations, resulting in the emergence of a new pattern of health and diseases (Hershkovitz *et al*., 1999). The industrial period is a pivotal age marking a shift towards increasing longevity, the chronic diseases associated with ageing, and a seeming rise in 'man-made' diseases (Western & Bekvalac, 2016). Although industrialisation generally improved living conditions, its economic consequences changed lifestyles significantly (Szeniczey *et al.*, 2019). Human population health has, however, undergone constant changes in response to environmental, nutritional, reproductive, and lifestyle changes throughout time (May *et al.*, 2011a). Environmental changes such as climate change and pollution (due to industrialisation) can lead to increased lifestyle-related diseases. Long-term air pollution exposure reduces bone mineral density (BMD) and increases bone fracture risk in later life (Prada *et al.*, 2023). The shift in dietary habits, such as increased consumption of dietary phytoestrogens, typically contained in foods such as soy, legumes, grains, and certain vegetables, has risen over the last decades (Raikos *et al.*, 2011). These food sources can affect oestrogen metabolism; however, increased bone density can benefit pre- and post-menopausal women (Raikos *et al.*, 2011). The estrogenic effect of these food sources is dose-dependent; thus, in societies with high consumption of phytoestrogens, the frequency of conditions such as HFI may be greater than in those with a more mixed food lifestyle (Cassidy & Faughnan, 2000). Changes in lifestyle and human fertility patterns, i.e., low birth rates, shorter periods of weaning, and extended reproductive periods, have increased oestrogen exposure, resulting in bone mass preservation (May *et al*., 2011). The emergence of lifestyle-related diseases, which are considered significant health changes, has led to a shift in medical research towards a better understanding of the causative factors, possible comorbidities, and short- and long-term complications. Thus, it is imperative to understand secular

changes in human health and microevolutionary changes seen in humans due to lifestyle and environmental changes.

Hyperostosis frontalis interna (HFI) is a long-standing, under-researched lifestyle-related disease (May *et al*., 2011a). HFI is a condition characterised by bony outgrowths located unilaterally or bilaterally on the intracranial surface of the anterior frontal bone (Devriendt *et al.*, 2005). HFI is generally restricted to the region between the skull midline and the superior sagittal sinus, while the middle meningeal artery's ascending branch acts as a barrier posteriorly (Hershkovitz *et al*., 1999). Patients diagnosed with HFI show thickening of the frontal bone caused by increased endocranial expansion of the diploë (Bracanovic *et al*., 2020). Although HFI mainly affects the frontal bone, some individuals may also present with increased bone thickness in other cranial bones, such as the parietal bone (Djonic *et al.*, 2016). HFI was often linked to obesity and hirsutism, as noted by Giovanni Batista Morgagni in 1719, the first to document the condition (Morgagni, 1719). Over two centuries later, Stewart (1928), Morel (1951) and Moore (1955) associated HFI with headaches, neuropsychiatric disorders, and hormonal imbalances, collectively naming it Morgagni-Stewart-Morel-Moore syndrome.

The variation in terminology associated with HFI reflects the ongoing debate regarding whether it represents a distinct pathological entity or is interconnected with other conditions characterised by cranial bone thickening, such as Hyperostosis Cranii Diffusa (HCD) and Hyperostosis Calvaria Interna (HCI) (Hershkovitz *et al.*, 1999). It is postulated that HFI and HCD represent different stages of a single pathological process, with HFI serving as an initial stage preceding the development of HCD (Moore, 1955). Perou (1964) introduced the term HCI to encompass all cases of endostosis, irrespective of their location within the endocranium, defining it as a slow, typically benign but occasionally progressive proliferation of bone affecting the inner table of the skull, particularly the frontal squama. Perou (1964) introduced the term HCI to encompass all cases of endostosis, irrespective of their location within the endocranium, defining it as a slow, typically benign but occasionally progressive proliferation of bone affecting the inner table of the skull, particularly the frontal squama. Perou (1964) also distinguished HCD as a primarily dystrophic and degenerative condition, not influenced by heredity, sex, or age, and lacking racial predilection or a specific clinical profile (Bracanovic *et al*., 2016).

It was concluded that HFI is a disease entity on its own, not a symptom of a broader syndrome, as suggested in the past (Hershkovitz *et a*l., 1999). While it can manifest in different forms, each is likely the outcome of the same underlying process and aetiology (Hershkovitz *et al*., 1999). Since HFI was first identified approximately 300 years ago, studies have endeavoured to reveal its prevalence, pathophysiology, and aetiology (May *et al*., 2010).

2. LITERATURE REVIEW

2.1. Prevalence of HFI in archaeological and modern populations

HFI has been reported to have a prevalence of between 5% and 12% in the general population, with an increasing prevalence in modern populations when compared to archaeological population groups, regardless of the geographical location of the population (Jaffe, 1972; Topaloğlu *et al.*, 2022). Thus, it remains uncertain whether HFI is a longstanding condition, or a relatively recent phenomenon influenced by lifestyle changes in the modern era (Bracanovic *et al*., 2016). Hershkovitz *et al.* (1999) analysed two series of skulls: 1,706 modern specimens from the 20th-century Hamann-Todd and Terry human osteological collections, which primarily represent individuals of European and African ancestry from the United States, and 2,019 pre-19th-century skulls from Central Europe, Amerindian populations, and the Eastern Mediterranean. Hershkovitz *et al.* (1999) observed a 12.8% incidence of HFI in a 20th-century sample from the Hamann-Todd and Terry human osteological collection. In contrast, no evidence of HFI was found in a 19th-century sample from East-Mediterranean, Amerindian, and Central European skulls. Hungary's skeletal collections dated between the 14th-century BC and the 17th-century AD, showed a 2.49% frequency of HFI (Hajdu *et al*., 2009). The overall frequency of HFI assessed on Ancestral Pueblans' skeletons was 32.4% (Mulhern *et al*., 2006), similar to the rate observed in populations from the last two centuries (Rühli *et al.*, 2004). Rühli *et al.* (2004) hypothesised that the similarities in frequency could be attributed to the comparable diet and lifestyle of the observed population (14th century BC to 17th century AD) with those of modern populations. This is because both populations lived in the ancient Pueblo Bonito house, which was believed to have been the

residence of predominantly wealthy people, supporting the hormonal model as the genesis factor of HFI (Rühli *et al.*, 2004).

Several hypotheses have been suggested to account for the higher frequency of HFI in modern populations (Rühli *et al.*, 2004). The observed increase in HFI prevalence may be linked to alterations in life expectancy (Rühli *et al.*, 2004). Lower life expectancy in historic times automatically means a lower prevalence of HFI in archaeological populations because the prevalence of this condition increases with age (Rühli & Henneberg, 2002). Hershkovitz *et al.* (1999) stated that females born in the early 9th century were more likely to develop HFI in their postmenopausal years, in contrast to its rarity in historical populations, where shorter lifespans led to a reduced postmenopausal period. Therefore, the Industrial Revolution represented a "turning point," resulting in longer lifespans and changes in female's lifestyles (Hershkovitz *et al.*, 1999).

It has been argued (Raikos *et al.*, 2011; May *et al.*, 2011b; Szeniczey *et al.*, 2019) that the increase in HFI in modern populations is due to lifestyle changes. Lifestyle changes, including a drastic decline in the number of children, shorter breastfeeding durations, and extended reproductive years due to earlier menarche and later menopause, contributed to hormonal imbalances in females (May *et al.*, 2011). In comparison to females who lived 100 years ago, modern females have nearly tripled the number of cycles during their reproductive years (Strassmann, 1999). The introduction to hormonal manipulation, such as contraceptives and hormonal replacement therapy, may also result in hormonal alterations in modern females (Stefanick, 2005). Lastly, a variety of contaminated agents, including the consumption of meat from hormone-treated animals (Andersson & Skakkebaek, 1999) and dietary phytoestrogens derived from sources such as soy, grains, and linseed (Cassidy & Faughnan, 2000) expose modern populations to exogenous hormones.

2.2. Sex and age distribution of HFI

In the modern era, the prevalence of HFI is relatively higher in females than males, with an estimated male-to-female ratio of 1:9 (Barber *et al*., 1997). While there is a higher prevalence in women, men also have been diagnosed with moderate HFI (She *et al.*, 2004). However, only men with hypogonadism and testicular atrophy had severe cases of HFI. (Raikos *et al*., 2011; Yamakawa *et al*., 2006). The variation in HFI distribution between sexes suggests that its severity is sex related (Hershkovitz *et al.*, 1999). The change in the prevalence between sexes is due to

lower birth rates in some populations and prolonged levels of higher oestrogen in women (Rühli *et al.*, 2004). These trends have also led many to postulate a link between HFI and sex hormone levels and their regulation (Rühli and Henneberg, 2002; Rühli *et al.*, 2004; May *et al.*, 2011b).

HFI has also been found to be more prevalent in elderly postmenopausal women in comparison to young females (Hershkovitz *et al.*, 1999). However, there seemed to be uncertainty about whether HFI shows increased progression with age within the individuals (Marlet, 1974). Moore (1955) proposed that HFI increases with age, while Marlet (1974) opposed the notion. Marlet (1974) suggested that even though HFI was more prevalent in individuals older than 50 years, age did not correlate with the severity of HFI. Similarly, it was shown by Nikolic *et al.* (2010) that older women had a higher probability of presenting with HFI; however, no association was observed between age and the extent of frontal bone involvement. Studies have shown that HFI can progress quickly from the onset and remain stagnant for several years, i.e., in patients over 70 years (Marlet, 1974; Hershkovitz *et al.*, 1999). HFI is an irregular process that, once initiated, may progress but can also stabilise or subside, as observed by Salmi *et al.* (1962). Salmi *et al.* (1962) observed through their analysis of radiological images of skulls across various age groups that the prevalence and severity of HFI peaked in individuals aged 40 to 60 years before rapidly diminishing. Ultimately, Hershkovitz *et al.* (1999) concluded that HFI is a sex-age-dependent phenomenon as it is notably less in males and females under 40 years of age, with severe cases occurring predominantly in females aged 60 years and above.

2.3. Aetiology of HFI

The aetiology of HFI is still unclear; however, the most likely cause has been attributed to hormonal changes and their impact on adult bone turnover/homeostasis (Bracanovic *et al.*, 2016). To better understand the potential causes driving changes in HFI frequencies over time, the relationship between sex steroids and bone mineral density should be explored (Riggs *et al.*, 2002). Oestrogen plays a critical role in preserving bone mass, regulating bone turnover, and maintaining balance between bone formation and resorption rates (Chow *et al*., 1992; Manolagas, 2000; Riggs *et al.*, 2002). Additionally, it influences the development, lifespan, and functional activity of osteoclasts and osteoblasts (Chow *et al*., 1992; Manolagas, 2000; Riggs *et al.*, 2002). Alterations in oestrogen levels lead to increased bone turnover, reduced bone mineral density, and overall disruption in bone remodelling, characterised by an extended resorption phase and a shortened

formation phase, ultimately contributing to osteoporosis (Christmas *et al*., 2002). Testosterone's primary function in bone metabolism is to reduce bone resorption and prolong the lifespan of osteoblasts and osteoclasts, and consequently increase the bone formation (Riggs *et al.*, 2002). Much of testosterone's function in the bone is through its aromatisation to oestrogen (May *et al*., 2011). Aromatisation refers to the enzymatic process by which aromatase converts testosterone into estradiol (Santen, 1975). While testosterone promotes the appositional bone growth at the periosteal surface, oestrogen counteracts this effect (May *et al*., 2011), therefore influencing the differences in skeletal morphology between sexes (Callewaert *et al*., 2010).

According to Perou (1964), endocrine imbalance, resulting from either congenital deficiencies or age-related deterioration, is the primary cause of HFI. Calame (1951) and Morel (1930) also proposed that dysendocrinism, caused by disturbances in gonadal function (such as impaired oestrogen stimulation, abnormal progesterone effects on the ovaries, or inadequate androgen stimulation by the testes), is a possible causative factor in the development of HFI. Calame (1951) and Morel (1930) further proposed that the disturbance of the tubero-infundibular region of the pituitary gland may contribute to the development of HFI, citing the similarity of symptoms associated with HFI and pituitary disturbances (e.g., adiposity, genital dystrophy, and disturbances in sugar metabolism).

Calame (1951) and Morel (1930) highlighted the role of gonadal factors, observing that male patients with HFI often exhibited signs of feminisation, including testicular atrophy. In contrast, Perou (1964) reported no evidence of feminisation in males with HFI but emphasised that testicular underdevelopment or atrophy was present in 5 out of 6 observed HFI cases. Males developed severe HFI as a result of extreme hormonal imbalances, such as testicular atrophy and consequently low testosterone levels (Yamakawa *et al*., 2006). Androgen suppression is the potential cause of the effects of oestrogen on bone metabolism. A study conducted by May *et al*. (2010) reported that males who underwent chemical castration as a treatment for prostate cancer experienced androgen suppression leading to an excess of oestrogen and an increased HFI occurrence.

Hershkovitz *et al.* (1999) proposed that HFI in females is likely caused by prolonged and/or increased oestrogen stimulation during the reproductive years. Historically, females spent much of their reproductive period either pregnant or nursing compared to modern females, resulting in

minimal oestrogen exposure, which likely contributed to the low prevalence of HFI in archaeological populations (Hershkovitz *et al.*, 1999). Interestingly, Hershkovitz *et al.* (1999) observed significant parallels between HFI and breast cancer, noting that increased or prolonged oestrogen stimulation is associated with an elevated risk of both conditions. Both cancer and HFI are predominantly observed in females, with their prevalence rising significantly after menopause. These conditions are linked to obesity and parity, with both the frontal bone and breast tissue known to be target tissues for hormones such as oestrogen and progesterone (Korenman, 1980).

Attanasio *et al.* (2013) hypothesised that one of the possible factors contributing to the aetiology of HFI is increased leptin levels. This peptide transmits signals of satiety to the hypothalamus and aids in the regulation of metabolic rate (Rühli & Henneberg, 2002). Rühli and Henneberg (2002) hypothesised that throughout human evolution, greater food availability favoured an increased leptin level and metabolic rate, potentially resulting in an increased occurrence of HFI. As leptin levels are strongly correlated to body mass index, Lahlou *et al*. (1997) postulated obesity as a form of primary resistance to circulating leptin, thus being associated with an increased incidence of HFI. Therefore, the oestrogen and leptin hypotheses are supported by the increased prevalence of HFI in the post-industrial era, which is associated with improved nutritional status (Murphy *et al.*, 2018). Additionally, HFI is thought to be associated with Type II diabetes mellitus and obesity (Bartelheimer, 1939; Rühli and Henneberg, 2002).

Genetic predisposition has emerged as a plausible aetiological factor in the development of HFI (Knies & Le Fever, 1941; McKusick, 1978; Rosatti, 1972; Watrous et al., 1993; and Glab *et al.*, 2006). Glab *et al.* (2006) described two females with HFI who were buried side by side within the family burial site; furthermore, they had the same measurements. The authors hypothesised that the two women were in a close kinship, and HFI could be a genetically determined alteration (Glab *et al.*, 2006). Watrous *et al.* (1993) described two males and one female with HFI. It was suggested that if the individuals of the 2300 mastaba group are closely related, this strengthens the suggestion of a genetic influence on the expression of HFI in males (Watrous *et al.*,1993). Lastly, environmental factors such as dietary phytoestrogens contribute to the development of HFI, particularly through their endocrine-modulating effects (Cassidy and Faughnan, 2000). Isoflavones and lignans found in soy, flaxseed, and various vegetables are known to influence oestrogen metabolism and may reduce bone loss, especially in pre- and postmenopausal women

(Mulhern *et al.*, 2006). The plant-based diet rich in phytoestrogens may have long-term hormonal effects on bone remodelling, supporting their role as a non-genetic, dietary risk factor in HFI aetiology (Mulhern *et al.*, 2006).

2.4. Pathogenesis of HFI

Throughout the years, various models have been proposed to explain the pathogenesis of HFI, namely the American, European, and Global models (Hershkovitz *et al.*, 1999). Moore (1955) described the “American model” of HFI as a process driven by the expansion of spongy bone, where an increase in diploic volume causes the inner table to shift toward endocranial structures. This model suggests that the outer table remains unaffected due to its greater thickness and structural durability (Moore,1955). The "European model," proposed by Thevoz (1966), defines HFI as a process occurring solely within the dura, initiated by the expansion of the intradural vasculature. The latest model, known as the "global model," proposed by Hershkovitz *et al*. (1999), suggests that HFI begins when osteogenic cells trigger a disorganised diploization process in the inner table. This process prompts the periosteum to deposit newly formed lamellae onto the inner table (Hershkovitz *et al.*, 1999). In the initial stages, this compact hyperostosis consists mainly of newly formed bone layers deposited by the dura (Hershkovitz *et al.*, 1999). As HFI progresses, blood vessels penetrate these layers, further stimulating bone growth. Over time, the original inner table becomes sclerotic, while the newly formed bone experiences extensive remodelling, resulting in the formation of large, irregular cavities known as blood sinuses (Hershkovitz *et al.*, 1999). These cavities contribute to the elevation of the endocranial plate, which is observed macroscopically as the characteristic overgrowth of HFI (Hershkovitz *et al.*, 1999). Finally, the inner table progressively undergoes resorption, while the remodelled bone expands into the diploic space and cranial cavity, ultimately leaving only a thin layer of lamellar bone enclosing the enlarged cavity (Hershkovitz *et al.*, 1999).

The global model suggests that the external plate and diploë remain unaffected, with the inward bulging of the inner table primarily resulting from the deposition of newly formed lamellar bone by the endosteal dura. (Hershkovitz *et al.*, 1999). The proposed model by Hershkovitz *et al.* (1999) contradicts Perou's (1964) assertion that the diploë is the main site of involvement, exerting pressure on the inner table from within. However, the strong adhesion of the dura to the inner

surface of the frontal bone provides support for both the European and global models (Hershkovitz *et al.*, 1999).

2.5.Diagnostic Imaging Technique

HFI expression has increased in modern times; however, it remains underdiagnosed mainly as it does not pose any immediate clinical symptoms but can impact brain volume (May *et al.*, 2012). The occurrence of HFI has been linked to a reduction in brain volume, suggesting a clear association between HFI and neurological disorders such as schizophrenia, Parkinson's disease and dementia (May *et al.*, 2012). Modern diagnostic imaging techniques, i.e., radiological (indirect) or macroscopic (direct) methods, have seen an increase in HFI diagnoses, which in turn may assist in better understanding the aetiology and progression of the condition (Cvetković *et al.*, 2020). Barber *et al.* (1997) reported that in the past, the prevalence of HFI was relatively low due to a lack of standard diagnostic criteria. Therefore, Barber *et al.* (1997) proposed to undertake a study to grade an archaeological sample of crania for HFI using exact radiological grading. The results obtained using this method indicated a notable increase in the prevalence of HFI among females in the archaeological population (Barber *et al.*, 1997), confirming the need for standardised scoring criteria in successfully diagnosing HFI. However, the main disadvantage of X-ray imaging is that this technique tends to overlook relatively mild cases (Rühli *et al.*, 2007).

The morphological manifestations of HFI differ in severity, ranging from small, discrete nodules to extensive overgrowth of the inner table of the frontal bone (Hershkovitz *et al.*, 1999). Hershkovitz *et al.* (1999) introduced a classification criterion using a systematic analysis, defining different types of HFI (Type A, B, C and D) based on the morphology and size of the affected area. This classification method predominantly relies on visual examination and manual measurement of osteological specimens. To accurately study the morphology and occurrence of HFI, it is essential to couple the classification criteria with advanced diagnostic imaging techniques. May *et al.* (2010) reported that plain radiological examination is unreliable for diagnosing HFI and thus proposed using Computerised Tomography (CT) imaging to identify and classify HFI. High-resolution 3D imaging, specifically micro-computed tomography (µCT), has been suggested as a possible solution to the limitations of other diagnostic tools (Rühli *et al.*, 2007). Micro-CT imaging allows for high-resolution visualisation of bone architecture without sample preparation or destruction in the area to be sectioned (Rühli *et al.*, 2007). This enables the

assessment of changes in the bone surface and alterations in the diploë at a micro-architectural level (Rühli *et al.*, 2007).

The first description of the micro-architecture of HFI examined by micro-CT was done by Rühli *et al*. (2007). The frontal bone, affected by HFI, showed a slowly progressing chronic process with no alterations on the outer table and external part of the diploic region. The overall density of the new tissue was increased (Rühli *et al.*, 2007). Rühli *et al*. (2007) did not include quantitative analysis in their study but outlined that three-dimensional visualisation could be beneficial in evaluating the size and type of HFI. However, they stressed that histological examination would be more useful because it better represents the texture of lamellar bone (Rühli *et al.*, 2007). Bracanovic *et al.* (2016) conducted a study analysing the three-dimensional micro-architectural patterns of HFI in aged women using micro-computed tomography. They found that the overall bone thickness and volume of the frontal bones increased in individuals presenting with HFI. This study showed the efficiency of this technique as a diagnostic tool (Bracanovic *et al*., 2020). Micro-CT is, however, not useful as a clinical diagnostic tool, given that micro-CT scanning cannot be performed on living individuals. (Rühli *et al.*, 2007). However, it proves highly valuable in forensic and archaeological samples, where it can provide detailed, non-invasive imaging of skeletal remains (Rühli *et al.*, 2007).

Despite the vast literature on HFI, ambiguity still exists in its aetiology, its prevalence in historical populations and across different demographic parameters, and its relationship to various comorbidities related to lifestyle changes. Biologically, the aetiology of HFI remains unclear, with ongoing debates about hormonal, genetic, and environmental influences (Raikos *et al.*, 2011; Hershkovitz *et al.*, 1999). Despite HFI's strong association with postmenopausal women, there is insufficient research on its occurrence in younger or male populations to establish comprehensive age- and sex-related variations (May *et al.*, 2011b; Cvetković *et al.*, 2020). Studies investigating HFI frequently relied on small, geographically constrained sample sizes, often limited to specific populations or historical periods. This methodological limitation significantly impacted the generalizability of findings and hindered the ability to identify global patterns in the condition's prevalence, morphology, and aetiology (Barber *et al.*, 1997; Hershkovitz *et al.*, 1999). Additionally, limited studies have compared the prevalence of HFI in ancient and modern

populations, restricting understanding of the environmental and genetic influences on its development over time (Hershkovitz *et al*., 1999).

Additionally, there is no consensus on diagnostic criteria for HFI, as methodologies vary widely, ranging from radiological imaging to macroscopic examinations. This lack of standardisation leads to inconsistencies in diagnosis and reporting (Barber *et al.*, 1997; Rühli *et al.*, 2007). Although advanced imaging techniques like micro-CT are more precise, they are underutilised, with some studies still depending on traditional radiology (Bracanovic *et al.*, 2016). Even when such technologies are used, they are rarely integrated with quantitative analyses to evaluate bone density and micro-architecture comprehensively (Rühli *et al.*, 2007). Expanding the scope of research to include diverse populations and more representative cohorts, while standardising diagnostic tools and incorporating quantitative analysis, is essential for developing a comprehensive understanding of HFI and addressing its demographical differences.

In South Africa, specific prevalence data for HFI in the general population or among subgroups are not well-documented. However, its appearance aligns with global patterns observed in postmenopausal populations and incidental findings during imaging studies. Further research into regional or demographic variations in South Africa could provide more localised insights. Given that HFI is a sex- and age-dependent phenomenon, it holds significant potential for applications in anthropological and forensic contexts, particularly aiding human identification. (Devriendt *et al.*, 2005; May *et al.*, 2011b). Its observation allows alignment with judicial evidence and enhances the precision of traditional methods for determining sex and age (Devriendt *et al*., 2005). Therefore, it is necessary to be familiar with this condition and its different forms (Devriendt *et al.*, 2005). Although the skull is the second-best sex and age indicator, it can still be utilised without the postcranial skeleton (Cvetković *et al.*, 2019).

3. AIMS AND OBJECTIVES

This study comprised two aims:

1. Assess the prevalence, expression, and severity of HFI in a South African skeletal sample using a morphological approach.

The objectives of this aim included:

- To assess the prevalence and types of HFI using Hershkovitz's *et al.*, (1999) morphological scoring criteria.
- To evaluate the applicability, reliability, and repeatability of the morphological scoring criteria.
- To investigate differences in HFI prevalence across age, sex, and populations.
- Assess the correlation between HFI severity and increasing age.

3. To gain insight into the aetiology and pathogenesis of hyperostosis frontalis interna by looking at the micro-architectural changes in affected cranial areas.

The objectives of this aim included:

- Use 3D-µCT visualisation to investigate possible quantifiable variations in the internal architecture (e.g., trabecular thickness and numbering) of cranial skeletal elements in a subsample of individuals presenting with HFI and those without.
- Assess the intra- and interobserver repeatability for the microarchitectural parameters.

4. MATERIALS AND METHODS

This study comprised two research phases. The first phase included an assessment of the prevalence and expression of HFI in a South African skeletal sample. In contrast, the second phase focused on understanding the aetiology and pathogenesis of HFI. Ethical clearance to utilise

skeletonised individuals for this study was obtained by applying for permission from the curator of the Raymond A. Dart Collection of Modern Human Skeletons as well as to the Head of the School of Anatomical Sciences for permission to use the ethics waiver obtained from the University of the Witwatersrand's Human Research Ethics Committee (HREC-medical, W-CBP-220504-01) (Appendix A).

4.1. Study sample

Adult crania were sourced from the Raymond A. Dart Collection of Modern Human Skeletons to assess the prevalence and expression of HFI. This collection is housed in the School of Anatomical Sciences at the University of the Witwatersrand in Johannesburg. The skeletal remains were mainly derived from unclaimed bodies from the regional hospitals and donors (Kramer *et al*., 2019), with many skeletons representing males (Dayal *et al*., 2009). The skeletal remains in the Dart collection are comprised of individuals from regional South African Black (72.78%), White (22.42%), Coloured (4.80%) and Indian (0.18%) populations. For this study, South African demographic census categories (namely African, White, Coloured and Indian) were used to highlight the population affinity of the samples.

Exclusion criteria for the entire samples included signs of any bone-related pathology on the cranium other than HFI (e.g., porotic hyperostosis, multiple myeloma, etc.), incompleteness (where the calotte may be missing or in cases where the calotte or frontal bones were damaged) and cases of severe antemortem cranial fracturing.

A total of 2186 adult crania, including both sectioned and complete crania, were assessed for morphological signs of HFI. Among the total individuals assessed, 669 were female, and 1517 were male. Of these, 375 individuals (17.15%) were found to present with HFI (Table 1), forming the study sample.

Table 1. Individuals assessed (n = 2186) and individuals presenting with HFI (n = 375) in the Raymond A. Dart Collection of Human Skeletons were sorted by population affinity, age, and sex. [1]

	Individuals assessed					Individuals presenting with HFI				
Sex	Age cohorts	SA Black	SA White	SA Coloured	Total	Age cohorts	SA Black	SA White	SA Coloured	Total
Females	20-29	73	2	4	**79**	20-29	10	0	1	**11**
	30-39	93	1	6	**100**	30-39	19	0	1	**20**
	40-49	78	7	9	**94**	40-49	26	2	5	**33**
	50-59	74	25	6	**105**	50-59	28	8	2	**38**
	60-69	57	60	6	**123**	60-69	27	24	1	**52**
	70-79	23	56	3	**82**	70-79	11	25	2	**38**
	80-89	10	64	1	**75**	80-89	8	34	0	**42**
	90+	3	8	0	**11**	90+	3	6	0	**9**
Total		**411**	**223**	**35**	**669**		**132**	**99**	**12**	**243**
Males	20-29	101	1	3	**105**	20-29	4	0	0	**4**
	30-39	223	4	10	**237**	30-39	9	0	1	**10**
	40-49	275	25	15	**315**	40-49	19	3	4	**26**
	50-59	270	36	14	**320**	50-59	19	3	2	**24**
	60-69	207	68	9	**284**	60-69	21	8	0	**29**
	70-79	72	71	10	**153**	70-79	3	18	1	**22**

	80-89	25	55	7	**87**	80-89	1	12	0	**13**
	90+	7	7	2	**16**	90+	1	3	0	**4**
Total		**1180**	**267**	**70**	**1517**		**77**	**47**	**8**	**132**
Grand total		**1591**	**490**	**105**	**2186**		**209**	**146**	**20**	**375**

[1] In the SA Indian population, 4 individuals were assessed, and zero individuals presented with HFI

To investigate the possible aetiology and pathogenesis of HFI using micro-CT scanning, a study and control sample were randomly selected from the original 375 individuals presenting with HFI and 2186 individuals assessed who did not present with any signs of HFI, respectively. A total of 30 adult crania sourced from Raymond A. Dart Collection of Modern Human Skeletons was used to assess the internal architecture and metric parameters of crania presenting with and without HFI (Table 2). The sample comprised 15 individuals with HFI (study sample) and 15 without HFI (control sample). Crania with the calotte removed were reassembled using low-density, non-metallic tape applied externally to maintain the correct anatomical orientation prior to micro-CT scanning.

Table 2. Micro-architectural sample (n = 30) representing age-at-death categories (10-year cohorts) for adult individuals in the Raymond A. Dart Collection of Modern Human Skeletons by population affinity and sex.

	HFI group					Control group				
Sex	Age cohorts	SA Black	SA White	SA Coloured	Total	Age cohorts	SA Black	SA White	SA Coloured	Total
Females	20-29	0	0	0	**0**	20-29	0	0	0	**0**
	30-39	1	0	0	**1**	30-39	0	0	0	**0**
	40-49	0	0	1	**1**	40-49	1	1	0	**2**
	50-59	0	0	1	**1**	50-59	1	1	0	**2**
	60-69	0	0	0	**0**	60-69	1	2	0	**3**
	70-79	0	0	1	**1**	70-79	0	1	0	**1**
	80-89	0	2	0	**2**	80-89	0	0	0	**0**
	90+	0	1	0	**1**	90+	0	0	0	**0**
Total		**1**	**3**	**3**	**7**		**3**	**5**	**0**	**8**
Males	20-29	0	0	0	**0**	20-29	0	0	0	**0**
	30-39	0	0	0	**0**	30-39	0	0	0	**0**
	40-49	2	0	1	**3**	40-49	2	0	0	**2**
	50-59	0	1	0	**1**	50-59	0	0	1	**1**
	60-69	1	0	0	**1**	60-69	1	1	0	**2**
	70-79	0	1	1	**2**	70-79	0	1	1	**2**
	80-89	0	0	0	**0**	80-89	0	0	0	**0**
	90+	0	1	0	**1**	90+	0	0	0	**0**
Total		**3**	**3**	**2**	**8**		**3**	**2**	**2**	**7**
Grand total		**4**	**6**	**5**	**15**		**6**	**7**	**2**	**15**

4.2. Morphological scoring criteria

To macroscopically assess the prevalence of HFI, morphological variation of the endocranial surface of the skull was examined using scoring criteria previously developed by Hershkovitz *et al.* (1999). In cases where the calotte was not removed, a light source was inserted through the foramen magnum to evaluate the degree of HFI. The Hershkovitz *et al.* (1999) scoring criteria used in this study served as a baseline for assessing the degree of HFI expression along with the location of bony outgrowths on the endocranial surfaces of the frontal bone surface (Fig 1).

Four types of HFI, representing different degrees of severity, are described as follows based on Hershkovitz *et al.* (1999) scoring criteria: "Type A represents isolated, elevated bony island(s), which may either present as single or multiple island(s). These may be observed unilaterally or bilaterally on the frontal bone and exhibited with discrete, often indented margins. These are generally under 10 mm in size and are commonly found on the anteromedial part of the frontal bone (Fig. 1). Type B is represented as nodular bony overgrowths without discrete margins and with only slight elevation identified on less than 25% of the frontal bone. Occasionally, isolated nodular areas can also be identified (Fig. 1). Type C: This is associated with more extensive nodular bony overgrowths, with irregular thickening of up to 50% of the frontal endocranial surface. A tendency for greater elevation and coalescence may be observed (Fig. 1). Type D: Represents continuous bony overgrowth involving more than 50% of the frontal endocranial surface. The entire region tends to be irregularly elevated with sharp, clearly demarcated borders (Fig. 1)".

To reinforce the reliability of the morphological analysis, 50 crania presenting with HFI were stratified according to their ordinal scale of expression.

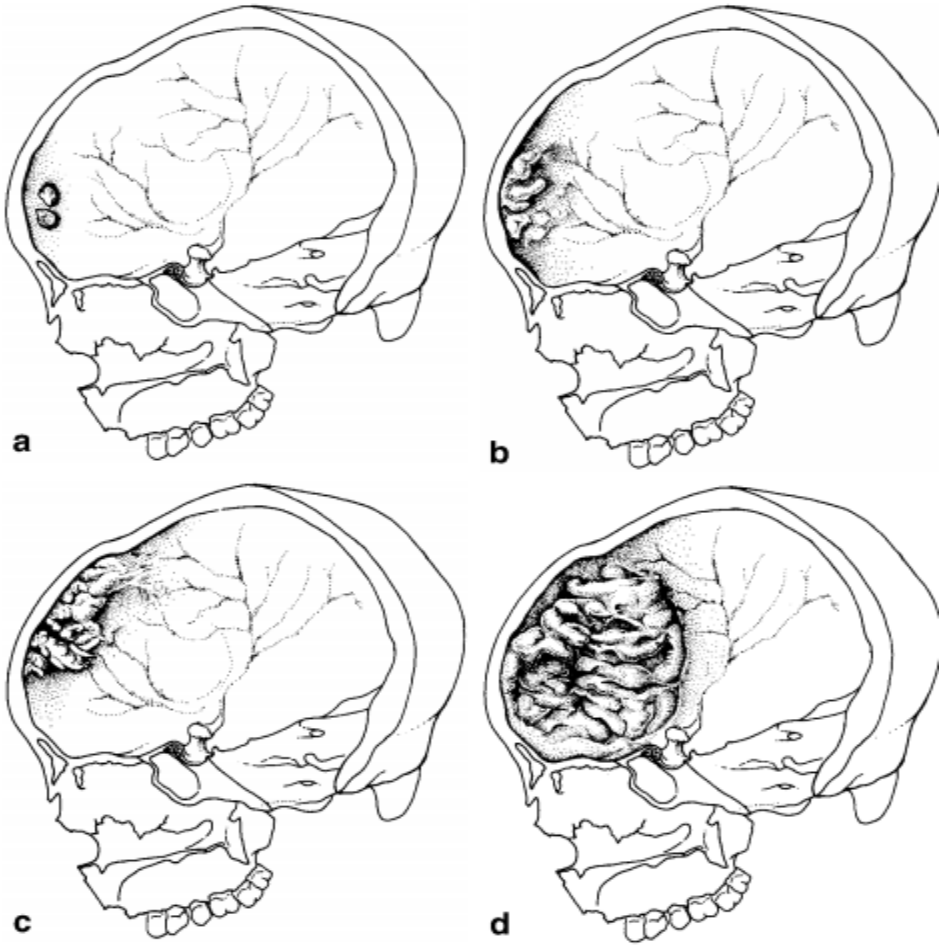


Figure 1: Schematic presentation of HFI types A–D relative to the endocranial surface of the human frontal bone extracted from Hershkovitz *et al*. (1999), pp.307 (Fig. 1. Schematic presentation of HFI types A–D).

4.3. Micro-architectural criteria

The selected 30 crania were subjected to micro-CT scanning to study the micro-architectural changes. All crania were scanned at the MIXRAD (Micro-focus X-ray Radiography and Tomography) facility at the South African Nuclear Energy Corporation (NECSA), using a Nikon XTH 225L Micro-CT X-ray unit (Nikon Metrology, Leuven, Belgium). The micro-CT scanning process was optimised for the highest possible spatial resolution by conducting "region of interest" scans. As such the scanning conditions ranged between 150kV/148 µm and 150kV/100 µm to compensate for the varying sizes of the crania. A 0.25 mm thick copper filter was used to optimise

X-ray penetrations through the crania. The crania were secured by mounting each in a polystyrene mould. Scanning at 360˚ was facilitated by placing the mounted crania on a rotating sample manipulator. The maximum magnification was used to improve the visualisation of the analysed structures. Immediately after scanning, slices were imported into the Nikon CTPro software (Nikon Metrology, Leuven, Belgium) package to reconstruct individual slices into volume files. The volume files were then imported into VGStudio max v3.2 (Volume Graphics GmbH, Heidelberg, Germany) for further analysis. Once imported into VG studio max v3.2, micro-CT scan volume files were subjected to a surface determination analysis to allow for the selection of fiducial landmarks on the skull.

Fiducial landmarks were selected along the sagittal plane of the cranium. They included the following landmarks: the glabella, anterior nasal spine and basion (Fig. 2). The selection of fiducial landmarks enabled the creation of a sagittal reference plane, which is essential to standardise the orientation of the micro-CT slices of the cranium. After the reference plane had been created, all slices were aligned to the sagittal plane of measurement (Fig. 2). Two additional planes were selected and aligned according to the most lateral point on the left and right lateral border of the nasal aperture, respectively, as well as the left and right infraorbital foramen (Fig. 2). These planes were aligned to specific cranial sites where HFI will be investigated, i.e., the lateral border of nasal aperture and infraorbital foramen (Fig. 2). The cranial sites were selected because they were easy to identify on the scan and enabled consistency in selecting and analysing the regions of interests between different individuals.

Regions of interest in each micro-CT scan were selected at the inferior border of the orbital fossa and the superior border of the frontal sinus on the left and right sides, respectively (Fig. 3). These areas were selected because they are most often affected by HFI (even in slight to moderate cases) (Djonic *et al.*, 2016).

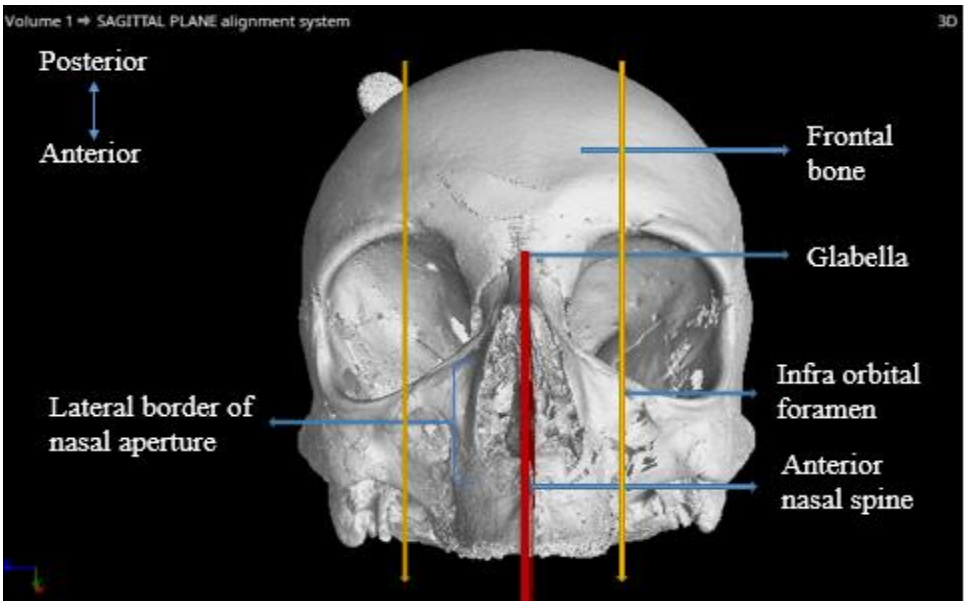


Figure 2. An anterior view of the cranium indicates the sagittal reference plane (red) established after selecting fiducial landmarks. Vertical lines (yellow) represent the sagittal planes aligned to the selected cranial sites of the frontal bone where regions of interest were selected.

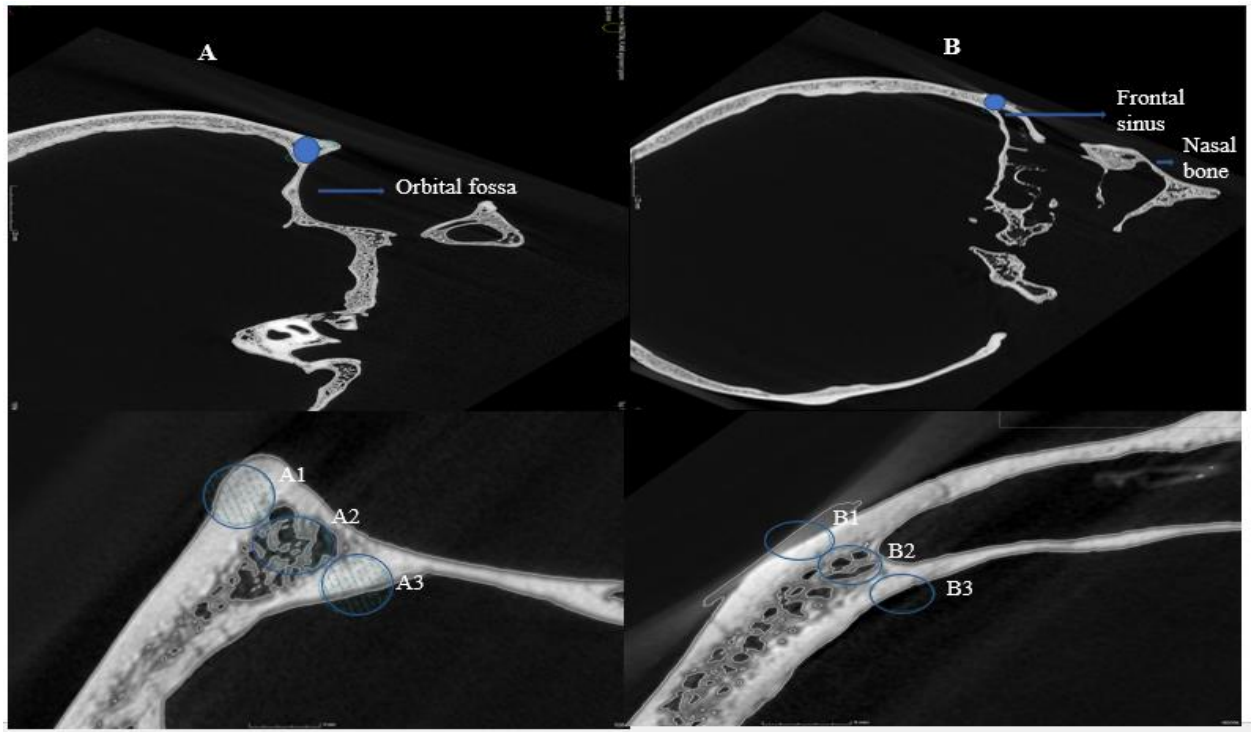


Figure 3. Micro-CT scans showing sagittal sections through the cranium at: A. infraorbital foramen, B. lateral nasal aperture (i.e., regions of interest). A1/A3/B1/B3 represent the cortical bone and A2/B2 represent the trabecular bone.

4.4. Micro-architectural parameters

Based on the regions of interest, micro-architectural parameters of both cortical and trabecular bone were investigated. To examine change in the proportion of bone density ($\frac{\text{Region of interest density}}{\text{reference material}}$), the density of each region was assessed on the extracranial (A1/B1), middle (A2/B2), and endocranial (A3/B3) surfaces. Each region of interest was set with a radius of 2*mm* and a thickness of approximately 1*mm* across the entire area. The selected diameters indicated the regions of interest without including redundant areas. A plastic density peg of uniform composition was included to act as a reference density material in assessing the proportional change of density across the sample.

To study the micro-architectural parameters of the trabecular region, related to A2/B2 (Fig. 3), the following measurements were taken: the bone volume fraction i.e., ratio of material (bone) volume to total volume ($\frac{\text{BV}}{\text{TV}}$); the corrected trabecular thickness (Tb.Th, mm), which specifies the mean thickness of trabecular structures in the material (bone) corrected for size, which was calculated as $\text{TbTh} = \frac{\frac{2}{\frac{\text{BS}}{\text{BV}}}}{}$, where $\frac{\text{BS}}{\text{BV}}$ is the ratio of material (bone) surface (BS) to material (bone) volume (BV) (Chen *et al.*, 2013). In addition, the mean trabecular number (Tb.N, 1/mm), which showed the mean number of trabecular structures per unit length, was calculated as $\text{TbN} = \frac{\frac{\text{BV}}{\text{TV}}}{\text{TbTh}}$; the mean trabecular spacing (Tb.Sp), indicating the mean distance between trabecular structures, which was calculated as $\text{TbSp} = \frac{1}{\text{TbN}} - \text{TbTh}$ (Chen *et al.*, 2013).

4.5. Statistical analysis

4.5.1. Morphological scoring method

A Shapiro-Wilk's was used to assess the normality of the sample, which further determined the statistical analyses to be conducted based on the data distribution type. Results from the normality tests indicated characteristics of both parametric and non-parametric distributions. To test the intra- and inter-observer reliability, the primary researcher and one independent researcher rescored the

morphological features of the 38 individuals' crania using Hershkovitz *et al.* (1999) criteria. The study's original scoring was compared to the primary researcher's second round of scoring and an independent researcher's scores. A weighted Cohen's Kappa test was used to test for repeatability. A weighted Cohen's Kappa results were interpreted as follows: values ≤ 0 as indicating no agreement and 0.01–0.20 as none to slight, 0.21–0.40 as fair, 0.60 as moderate, 0.61–0.80 as substantial, and 0 1.00 as almost perfect agreement (McHugh, 2012).

The following statistical tests were performed i.e., descriptive statistics and frequencies, to illustrate the distribution of HFI in the study sample. Given the non-parametric distribution of the data (Appendix B), Spearman's correlation coefficient test was used to assess the correlation of HFI with age between sexes and population groups. Correlation coefficients (r) were interpreted as follows: a coefficient (r) in the range of 0.00 to 0.10 indicated negligible correlation, 0.10 to 0.39 suggested weak correlation, 0.40 to 0.69 implied moderate correlation, 0.70 to 0.89 indicated strong correlation and 0.90 to 1.00 represented a very strong correlation (Schober *et al*., 2018). Fisher's exact test was used to compare HFI types between sexes. Chi-squared tests were used to statistically evaluate the differences between HFI frequencies across population groups and age cohorts, as the data satisfied the assumptions for parametric statistical analysis (Appendices C and D). Post hoc testing (one-way ANOVA) was used to assess the statistical differences between and within population groups statistically. All statistical tests were run using the SPSS version 23.0 software package (IBM).

4.5.2. Micro-architecture

A Shapiro-Wilk test was used to assess the normality of micro-architectural data distribution (Appendix E). Since the data were quantitative, inter- and intra-observer errors were assessed through repeated measurements on 10 randomly selected individuals, using Lin's concordance correlation coefficient (Lin's CCC) to evaluate reproducibility. All statistical analyses were performed in R Studio. This provided information on the method's level of repeatability and the degree of association between measurements (Allan, 1982). Lin's CCC results were interpreted according to McBride (2005). McBride (2005) classified Lin's CCC as follows: <0.90 indicates poor agreement, 0.90–0.95 moderate, 0.95–0.99 substantial, and ≥0.99 almost perfect agreement.

A paired sample T-test was used for parametric variables and the Wilcoxon Signed-Rank Test for non-parametric variables to assess the differences between the left and right measurements. The Independent sample T-test and Mann-Whitney test were used to assess the differences in mean values of all tested variables between males and females in the HFI and control groups. Pearson's correlation coefficient test was used to assess the correlation in changes in parameter mean values with increasing age in the HFI and control group and between males and females within both the HFI and control groups. No significant tests were done to compare the population differences in HFI and control groups and the severity of HFI due to the small sample size (n = 15). Statistical parameters (i.e. standard deviation, mean, median, min and max) were obtained via descriptive statistics for each measurement (SPSS 23.0) with a 0.05 significance level. A Bonferroni correction was applied to account for multiple comparisons and reduce the risk of Type I error.

5. RESULTS

5.1. HFI expression in the sample

HFI was observed in 17.15% (n = 375) of the cranial vaults assessed (n = 2186) in the Raymond A. Dart Collection of Modern Human Skeletons (Appendix F). Four types of HFI were observed with slight variations to the original criteria set out by Hershkovitz *et al.* (1999). The following observations and amendments to the scoring criteria were made during the data analysis.

Crania presenting with HFI type A showed single to multiple isolated nodules situated unilaterally or bilaterally on the intracranial surface of the anterior frontal bone (Fig. 4). The nodules observed were generally under 10 mm in size; however, in some cases, they were greater than 10 mm (Fig. 4b). In some type A cases, bony outgrowths observed had no discrete margins (Fig. 4b).

Type B demonstrated multiple nodules situated bilaterally on the frontal bone (Fig. 5). The outline of nodules was less well-defined, with a general decrease in the outgrowth elevation towards the sagittal suture (Fig. 5a). However, in some cases, slight elevation of the nodules could still be observed (Fig. 5b).

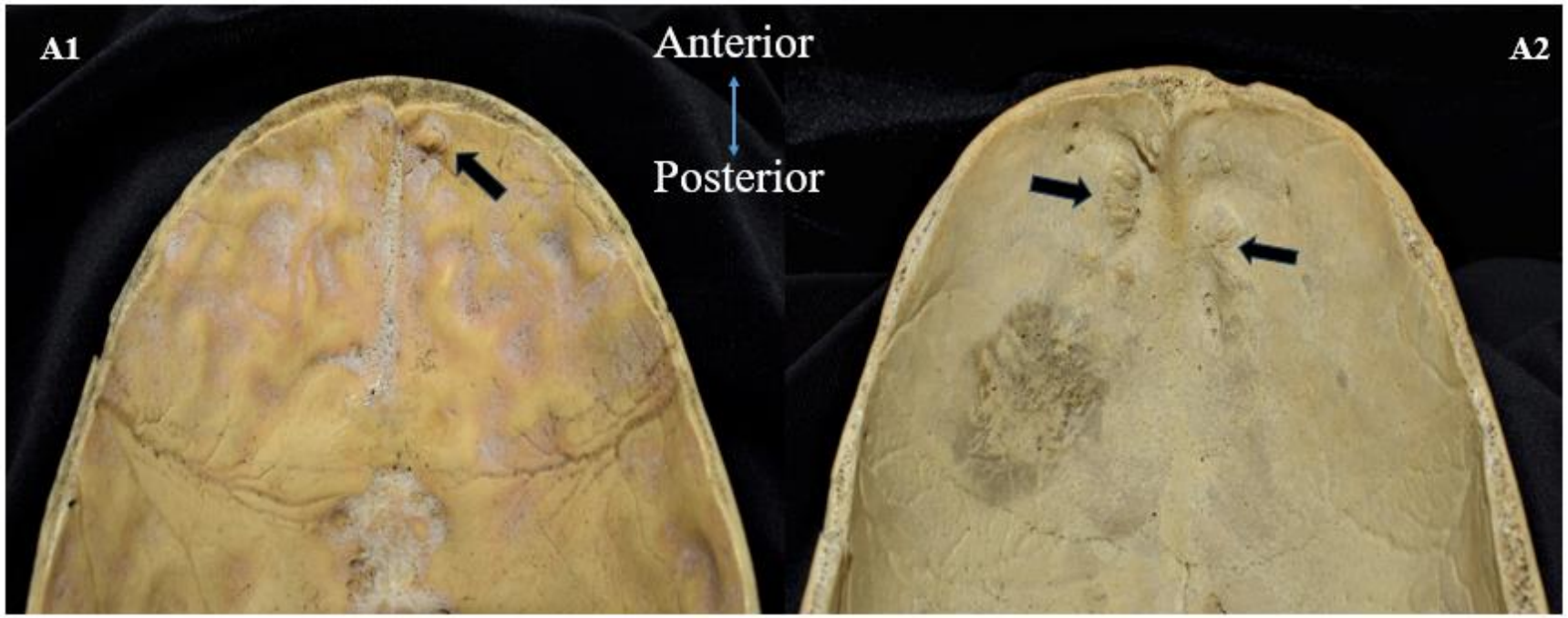


Figure 4. Intracranial views of skulls presenting with HFI Type A showing an isolated, elevated bony island(s), single (A1) or multiple (A2), unilateral (A1) or bilateral (A2), all with discrete, often undermined margins (arrows). Image A1 represents a 61-year-old SA Black male, and A2 is a 45-year-old SA Black male.

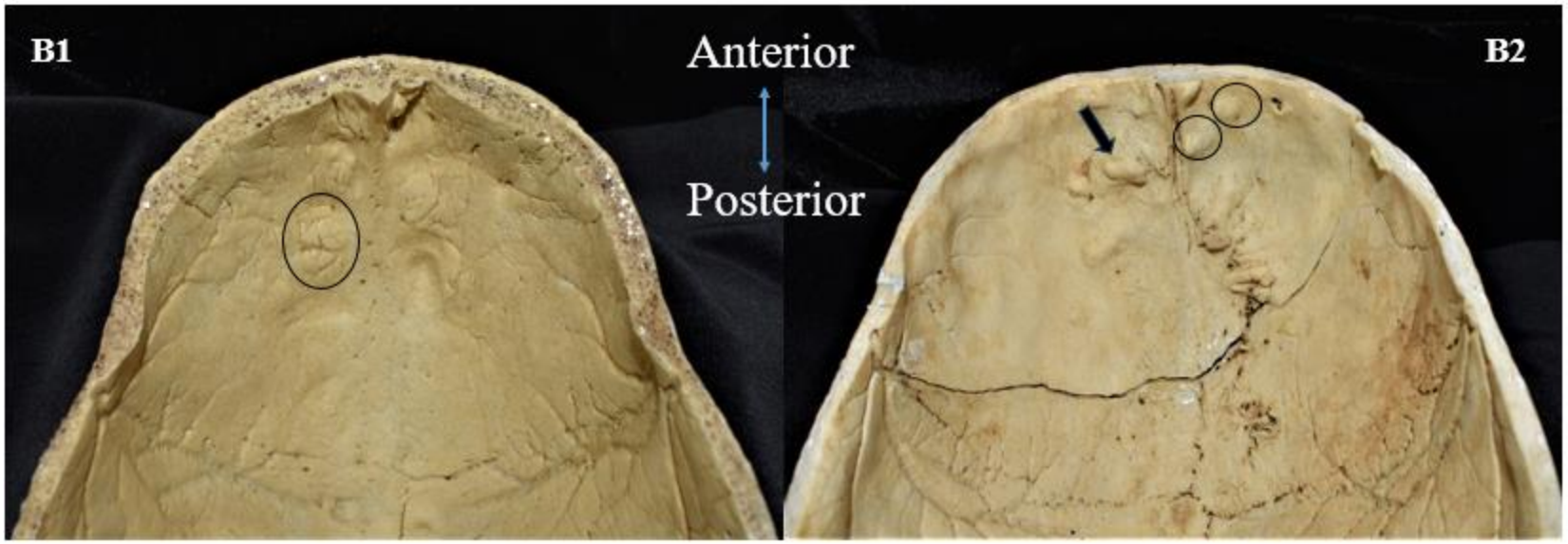


Figure 5. Intracranial views of skulls presenting with HFI Type B show a bony overgrowth(s) without discrete margins (oval (B1)) and slight elevation (arrow (B2)). Occasionally, isolated nodular areas were also identified (circles). Image B1 represents a 46-year-old SA Coloured Female, and B2, a 63-year-old SA White female.

Type C was associated with the coalescence of bony nodules and irregularity of up to 50% of the frontal bone. For Type C, an increased elevation was not necessarily observed but instead was characterised by marked expansion of coalesced nodules and irregular thickening of the frontal bone (Fig. 6).

Crania presenting with HFI Type D was associated with extensive thickening and increased coalesced bony outgrowths, and in some areas, thickening resembling striations (Fig. 7a). The characteristic cauliflower appearance could be observed in most cases (Fig. 7b). In some cases, osseous thickening extended beyond the frontal bone to include the parietal and temporal bones of the endocranial surfaces. These cases are normally classified as Hyperostosis Cranii Interna (HCI) and were not included in the original scoring criteria. In this study, when HCI was identified, the crania were classified as Type D. Bony formations in the form of ridges and grooves were found to be oriented perpendicularly and obliquely to the midsagittal plane. HFI did not affect suture lines, even in severe cases. HFI was consistently absent in the skull midline and superior longitudinal sinus. The ascending branch of the middle meningeal artery groove was spared in the rare cases where parietal thickening was also observed (Fig. 7a).



Figure 6. An intracranial view of the skull of a 48-year-old SA Black male presenting with HFI Type C showing the expansion of coalesced nodules and irregular thickening of the frontal bone (arrows).

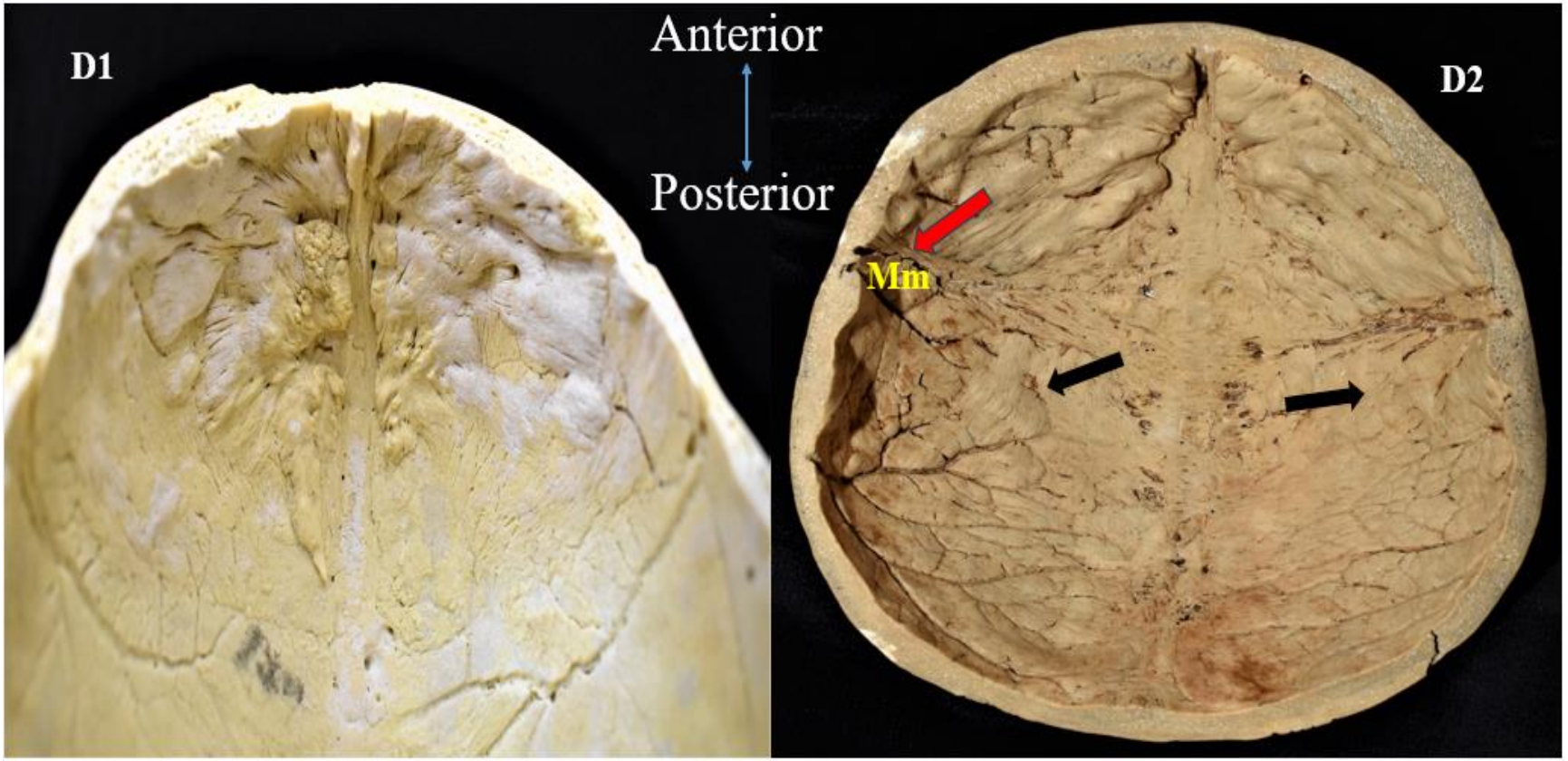


Figure 7. An intracranial view of skulls presenting with HFI Type D is characterised by extensive thickening of the intracranial surface extending to the parietal and temporal bones (black arrows (D2)). Type D exhibits clustered lobulations or a cauliflower shape (D2). Image D1 represents an 85-year-old SA White female, and D2 in an 82-year-old SA White female. Mm (red arrow) represents the middle meningeal artery groove.

5.2. Intra- and inter-observer reliability

The reliability tests for HFI scoring were calculated using a weighted Cohen's kappa. The analysis of intra-observer showed a strong level of agreement, $k = 0.891$ ($P < .001$), while inter-observer showed a moderate level of agreement, $k = 0.713$ ($P < .001$).

5.3. Distribution of HFI according to sex and population affinity

HFI Type A was most prevalent (n = 130/375, 34.7%), followed by Type B (n = 127/375, 33.9%) and Type C (n = 65/375, 17.3%). The lowest number of individuals presented with Type D (n = 53/375, 14.1%).

Overall, a significantly higher prevalence of HFI was observed in females (n = 243/375, 64.8%) compared to males (n = 132/375, 35.2%), as determined by Fisher's exact test ($p \leq 0.01$). When taking types of HFI into account, it was noted that Type A was slightly more prevalent in males (n = 70/130, 53.8%) than in females (n = 60/130, 46.2%) (Fig. 8) (Appendices G and H). Conversely, Types B, C and D respectively were more prevalent in females (B: n = 91/127, 71.7%; C: n = 49/65, 75.4%; D: n = 43/53, 81.1%) when compared to males (B: n = 36/127, 28.3%; C: n = 16/65, 24.6%; D: n = 10/53, 18.9%). However, these differences were not statistically significant (p = 1.000).

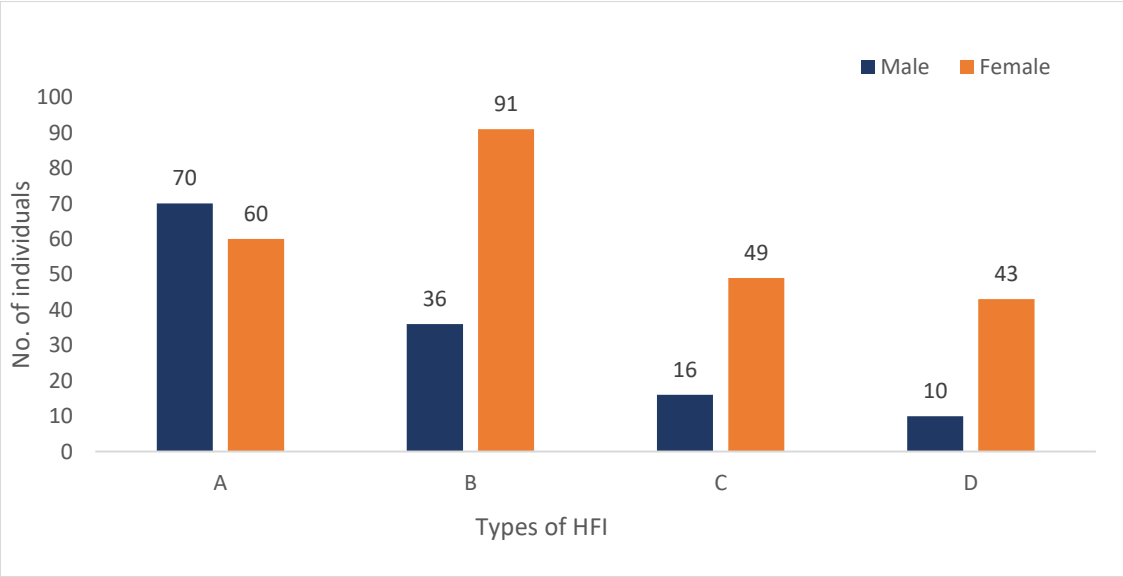


Figure 8. Distribution of females and males presenting with various types of HFI.

South African Black individuals (n = 209/375; 55.73%) presented with a higher frequency of HFI compared to the SA White (n = 146/375; 38.93%) and SA Coloured individuals (n = 20/375; 5.33%), respectively (Fig. 9). There was a statistically significant difference between population groups as determined by a one-way ANOVA (F (2,372) = 5.353, P = 0.005). A Tukey's post hoc test indicated that within the population groups, a significant difference was specifically observed between the SA Black and SA White individuals (p = 0.013), with a higher prevalence of HFI among SA Black individuals. In contrast, no significant differences were observed between the SA Coloured (and the SA White population (p = 0.056) and between SA Coloured and SA Black populations (p = 0,551). No cases of HFI were observed in the SA Indian sample (n = 4) and were therefore excluded from the study sample. A significant difference in the distribution of HFI types among the different South African population groups was observed (X = 12.98; p = 0.043). Types A, B, and C were more common in the SA Black sample (A: n = 78/130, 60%; B: n = 74/127, 58.27%; C: n = 36/65, 55.38%) as compared to SA White (A: n = 41/130, 31.54%; B: n = 48/127, 37.80%; C: n = 27/65, 41.54%) and SA Coloured individuals (A: n = 11/130, 8.46%; B: n = 5/127, 3.94%; C: n = 2/65, 3.08%) (Fig. 9). However, Type D, the most advanced stage, was more prevalent in the SA White sample (n = 30/53, 56.60%) (Fig. 9).

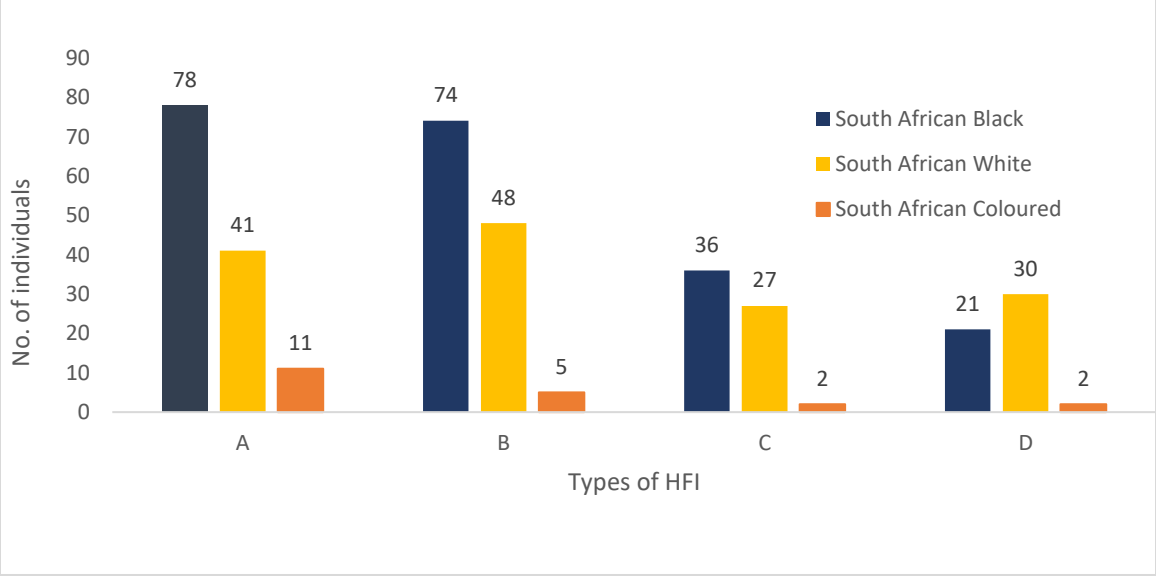


Figure 9. Distribution of South African Black, South African White and South African Coloured samples presenting with various types of HFI.

In the SA White sample, HFI was observed significantly more (X = 11.002; p = 0.12) in females (n = 99/146, 67.80%) than in males (n = 47/146, 31.19%). All types of HFI were more prevalent in SA White females (A: n = 21/41, 51.22%; B: n = 31/48, 64.58%; C: n = 22/27, 81.48%; D: n = 25/30, 83.33%) as compared to SA White males (A: n = 20/41, 48,78%; B: n = 17/48, 35.42%; C: n = 5/27, 18.52%; D: n = 5/30, 16.67%). The distribution of HFI Types B (X = 5.382; p = 0,02), C (X = 14.392; p < 0.001), and D (X = 16.772; p < 0.001) showed significant differences between males and females in the SA White sample. No significant difference was observed in Type A (X = 0.002; p = 0.82).

In the SA Black sample, HFI was observed significantly more (X = 17.978; p ≤ 0.001) in females (n = 132/209, 63.16%) than in males (n = 77/209, 36.84%). Type A was more prevalent in SA Black males (n = 43/78, 55.13%) than in SA Black females (n = 35/78, 44.87%); however, Types B, C and D were more prevalent in SA Black females (B: n = 55/74, 74.32%; C: n = 26/36, 72.22%; D: n = 16/21, 76.19%) when compared to SA Black males (B: n = 19/74, 25.68%; C: n = 10/36, 27.78%; D: n = 5/21, 23.81%). The distribution of HFI Types B (X = 28.783, p < 0.001), C (X = 16.728, p < 0.001), and D (X = 8.529; p < 0.001) showed significant differences between males and females in the SA Black sample, with females more often presenting with these types. No significant difference was observed in Type A (X = 1.315; p = 0.25).

In contrast, no statistical difference between sexes was observed in SA Coloured individuals (X = 7.311; p = 0.063). However, the frequency of HFI was somewhat higher in SA Coloured females (n = 12/20, 60%) than SA Coloured males (n = 8/20, 40%). South African Coloured males (n = 7/11, 63.64%) presented with a high frequency of HFI Type A compared to SA Coloured females (n = 4/11, 36.36%). Type B and D were not observed in SA Coloured males; however, in SA Coloured females, five and two individuals presented with Type B and D, respectively. Type C was similarly distributed in both SA Coloured males and females (n = 1/2, 50%; n = 1/2, 50%). No significant differences were observed for any HFI types between males and females in the SA Coloured population (Type A: X = 1.636, p = 0.201); B: X = 2.950, p = 0.086; C: X = 0.0, p = 1.0 and D: X = 2.112, p = 0.146).

5.3.1. Distribution of HFI according to age

HFI was more prevalent among individuals aged 50-69 years (n = 143/375; 38.13%), followed by the 70+ years (n = 128/375; 34.13%) and 20-49 years (n = 104/375; 27.73%) groups respectively. No significant difference was observed between age cohorts and HFI, as indicated by Chi- squared test (X = 12.124; p = 0.059). Within the age cohorts, Types A, B and C were more prevalent in middle-aged individuals, i.e., 50-69 years (A: n = 49, 13.06%; B: n=50, 13.33%; C: n=28, 7.46%) (Fig. 10). Type D was more prevalent in older-aged individuals, i.e., 70+ years (n = 128; 34.13%) (Fig. 10). There was a weak positive correlation between HFI and increasing age (rho (ρ) = 0.150, p = 0.004) (Fig 11).

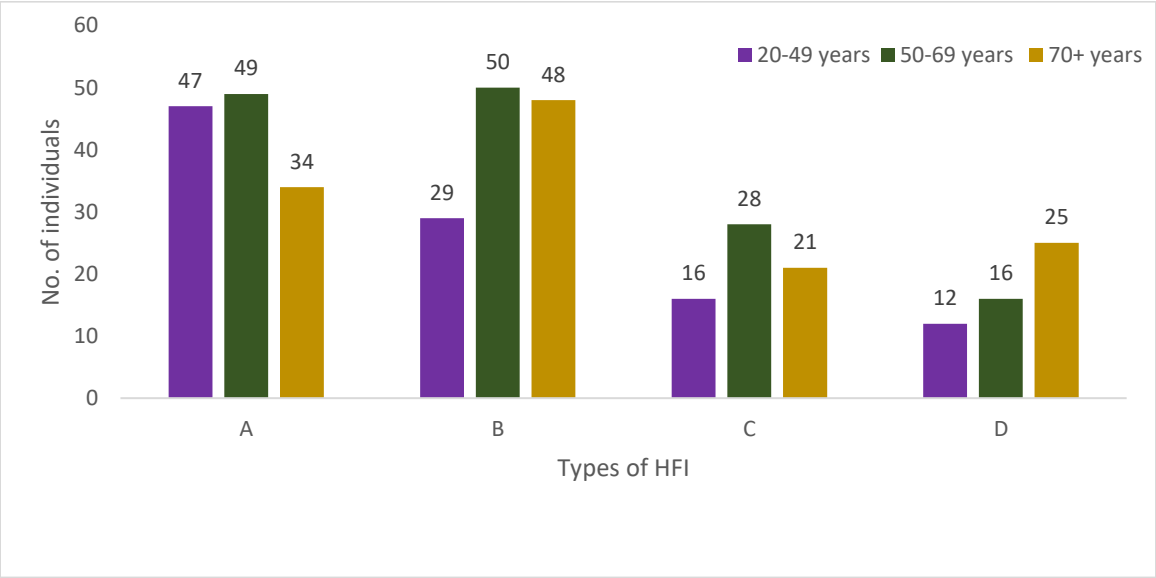


Figure 10. Distribution of individuals presenting with various types of HFI in different age cohorts i.e., 20-49 years (young age), 50-69 years (middle age) and 70+ years (old age).

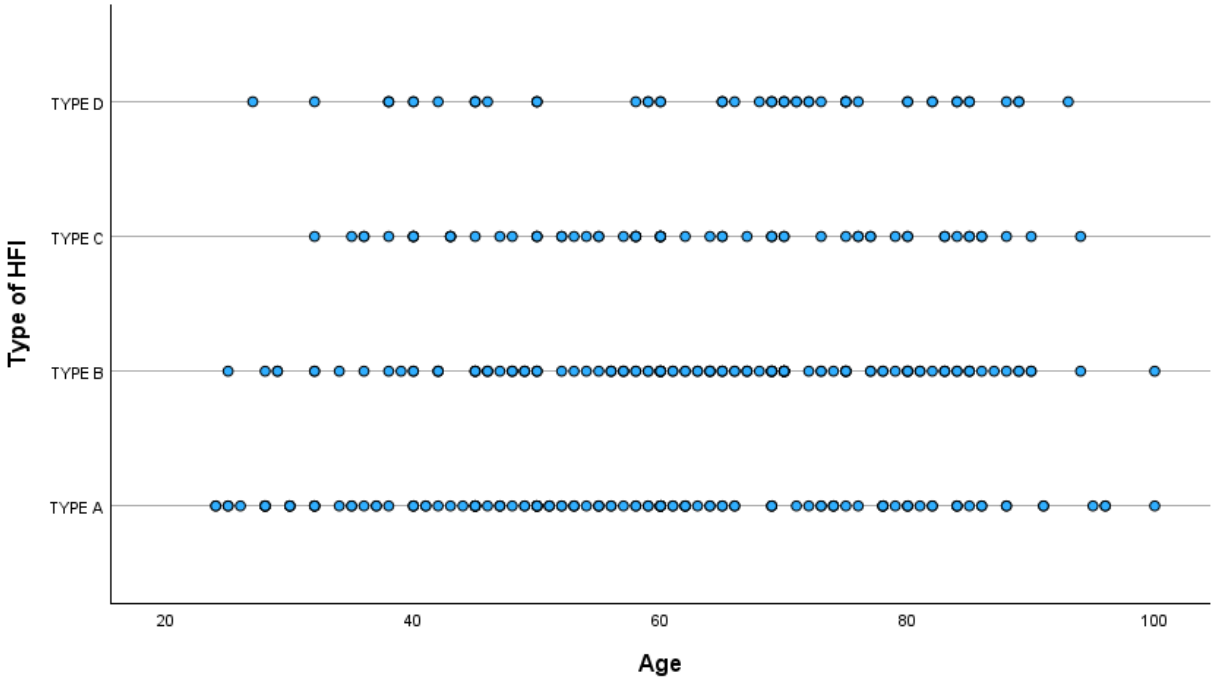


Figure 11. A Scatter plot indicating the correlation between age and the severity of HFI.

Distinct patterns in the frequency of HFI between females and males across different age groups were observed. The frequency of HFI in females increased with age and remained relatively stable between the middle- and older-aged groups: 20-49 years (n = 64/243, 26.33%), 50-69 years (n = 90/243, 37.03%) and 70+ years (n= 89/243, 36.6%). In male individuals, the frequency of HFI increased from younger (n = 40/132, 30.30%) to middle-aged (n = 53/132, 40.15%) individuals, with a decreasing frequency between middle-aged to old-aged (n = 39/132, 29.55%) individuals. A weak positive correlation was observed in both males (rho (ρ) = 0.122) and females (rho (ρ) = 0.152) when age and the degree of HFI were considered.

The frequency of HFI across the SA White sample increased with age, i.e., young age (n = 5/146, 3.42%), middle age (n = 43/146, 29.45%) and old age (n = 98/146, 67.12%). In the SA Coloured sample, the frequency of HFI decreased with age, i.e., young age (n = 12/20, 60%), middle age (n = 5/20, 25%) and old age (n = 3/20, 15%). In the SA Black sample, the frequency of HFI increased from young-aged (n = 87/209, 41.62%) to middle-aged (n = 95/209, 45.45%) and then decreased during older-aged (n = 27/209, 12.92%) individuals. When considering age and the degree of HFI, both the SA Black (rho (ρ) = 0.081) and SA White individuals (rho (ρ) = 0.073) showed a weak

positive correlation. In contrast, the SA Coloured showed a negative, weak correlation (rho (ρ) = - 0.117).

In the assessment of sex differences among population samples, the frequency of HFI in SA Black males increased from young-aged (n = 32/77, 41.56%) to middle-aged (n = 40/77, 51.95%), with a decrease between middle-aged to older-aged (n = 5/77, 6.49%) individuals. In contrast, in females, it decreased with increasing age, i.e., young age (n = 55/132, 41.67%), middle age (n = 55/132, 41.67%) and old age (n = 22/132, 16.67%). A weak positive correlation was observed in both SA Black males (rho (ρ) = 0.126) and females (rho (ρ) = 0.046). In SA Coloured individuals, the frequency of HFI for males decreased with age (young age: n = 5/8, 62.5%; middle age: n = 2/8, 25%; old age: n = 1/8; 12.5%). Similarly, the frequency of HFI for females in the SA Coloured sample decreased with age (young age: n = 7/12, 58.33%; middle age: n = 3/12, 25%; old age: n = 2/12; 16.67%). A moderate negative correlation was observed in SA Coloured males (rho (ρ) = - 0.592), whereas females showed a weak positive correlation (rho (ρ) = 0.006). In SA White individuals, the frequency of HFI for males increased with age (young age: n = 3/47, 6.38%; middle age: n = 11/47, 23.40%; old age: n = 33/47 70.21%). Similarly, the frequency of HFI for females in the SA White sample increased with age (young age: n = 2/99, 2.02%; middle age: n = 32/99, 32.32%; old age: n = 65/99; 65.66%). A weak negative correlation was observed in SA White males (rho (ρ) = -0.193), whereas females showed a weak positive correlation (rho (ρ) = 0.185).

5.4. Intra- and inter-observer reliability for the microarchitectural parameters

A poor strength of agreement was observed in all measurements of intra-observer with the exception of trabecular spacing (Tbsp), which achieved perfect agreement (Table 3). Similarly, all measurements of the inter-observer within the study showed a poor strength of agreement (Table 3).

Table 3. An overview of intra- and inter-observer repeatability results using Lin's concordance correlation coefficient (Lin's CCC), with the estimated CCC values and their corresponding 95% confidence intervals (CI).

Parameter	Intra-Observer CCC (95% CI)	Inter-Observer CCC (95% CI)
Minimum Density	0.53 (0.39 – 0.65)	- 0.01 (- 0.14 – 0.11)
Mean Density	0.59 (0.46 – 0.69)	- 0.05 (- 0.21 – 0.11)
Maximum Density	0.34 (0.18 – 0.48)	0.57 (0.45 – 0.67)
BVTV	0.34 (0.18 – 0.48)	0.02 (- 0.07 – 0.11)
BSBV	0.37 (0.28 – 0.46)	0.56 (0.44 – 0.65)
TBTH	0.38 (0.23 – 0.51)	- 0.00 (- 0.01 – 0.01)
TBN	- 0.01 (- 0.02 – 0.01)	- 0.00 (- 0.02 – 0.01)
TBSP	1.00 (1.00 – 1.00)	- 0.00 (- 0.02 – 0.01)

BS/BV, bone surface to bone volume; BV/TV, bone volume to tissue volume; TBN, trabecular number; TBSP, trabecular spacing; and TBTH, trabecular thickness.

5.5. Micro-architectural differences between individuals with and without HFI

No significant differences were observed between the left and right measurements; as such, the values of the investigated parameters were averaged to provide the overall values for the cortical and trabecular regions.

In individuals with HFI, notable differences were observed in various micro-architectural parameters compared to individuals without HFI. Individuals with HFI had an increased bone mineral density and bone-surface-to-bone-volume ratio (BS/BV) across the infraorbital foramen (Table 4) and lateral nasal aperture (Table 5) in both cortical and trabecular regions compared to those without HFI. Although the mean bone mineral density and bone-surface-to-bone-volume ratio (BS/BV) values were higher in individuals with HFI, the differences between the groups were not statistically significant (Tables 4 & 5). Furthermore, individuals with HFI demonstrated a decreased bone-volume-to-tissue-volume ratio (BV/TV) across the infraorbital foramen (Table 4) and lateral nasal aperture (Table 5) in both cortical and trabecular regions compared to those without HFI. No significant difference in the bone-volume-to-tissue-volume ratio (BV/TV) was

observed between individuals with HFI and those without HFI across the infraorbital foramen and lateral nasal aperture in both cortical and trabecular regions (Tables 4 & 5).

When comparing trabecular bone-related micro-architectural parameters, individuals with HFI had a decreased trabecular thickness (TBTH) in both the infraorbital foramen (Table 5) and lateral nasal aperture (Table 5) compared to those without HFI, with significant differences found only in the infraorbital foramen ($p = 0.033$). Individuals with HFI had an increased trabecular number (TBN) across the lateral nasal aperture region compared to those without HFI (Table 5). Although the mean trabecular numbers (TBN) were higher in individuals with HFI, the differences between the groups were not statistically significant (Table 5). Conversely, individuals with HFI had a decreased trabecular number (TBN) across the infraorbital region compared to those without HFI (Table 3). However, this difference was not statistically significant (Table 4). Individuals with HFI had an increased trabecular spacing (TBSP) across the infraorbital region compared to those without HFI, however, no significant difference was observed (Table 4). When looking at the trabecular spacing (TBSP) across the lateral nasal aperture, the mean values were equal between those who presented with and without HFI, and no significant difference was observed (Table 5).

Table 4. Micro-architectural parameters in individuals with and without HFI (SD - standard deviation) across the infraorbital foramen region.

Micro-architectural parameter	Individuals with HFI *N* = 15 (Mean ± SD)	Individuals without HFI *N* = 15 (Mean ± SD)	*P*-value
Cortical bone			.
DA1	62529.03 ± 4203.28	60990.1 ± 4994.66	0.44
DA3	61994.93 ± 5192.22	60620.5 ± 5640.84	0.40
BV/TVA1	0.75 ± 0.19	0.81 ± 0.21	0.25
BV/TVA3	0.52 ± 0.13	0.57 ± 0.22	0.43
BS/BVA1	0.63 ± 0.43	0.61 ± 0.44	0.89
BS/BVA3	1.51 ± 0.61	1.09 ± 0.62	0.25
Trabecular bone			
DA2	59941.27 ± 6194.45	59750.47 ±6351.11	0.88
BV/TVA2	0.69 ± 0.27	0.73 ± 0.18	0.98
BS/BVA2	3.1 ± 2.84	1.99 ± 1.41	0.51
TBTHA2	0.69 ± 0.94	1.53 ± 1.52	**0.03 ***
TBNA2	0.61 ± 0.38	0.67 ± 0.31	0.64
TBSPA2	0.38 ± 0.34	0.36 ± 0.13	0.33

D, density; BS/BV, bone surface to bone volume; BV/TV, bone volume to tissue volume; TBN, trabecular number; TBSP, trabecular spacing; and TBTH, trabecular thickness. A1 denotes extracranial, A2 middle, and A3 endocranial surfaces. ***p<0.05**.

Table 5. Micro-architectural parameters in individuals with and without HFI (SD - standard deviation) across the lateral nasal aperture region.

Micro-architectural parameter	Individuals with HFI *N* = 15 (Mean ± SD)	Individuals without HFI *N* = 15 (Mean ± SD)	*P*-value
Cortical bone			
DB1	63054.1 ± 3107.98	61019.93 ± 5202.36	0.46
DB3	62325.97 ± 4168.35	60788.47 ± 5195.8	0.41
BV/TVB1	0.61 ± 0.19	0.75 ± 0.2	0.07
BV/TVB3	0.53 ± 0.17	0.62 ± 0.21	0.22
BS/BVB1	0.83 ± 0.4	0.65 ± 0.47	0.28
BS/BVB3	1.24 ± 0.49	1.04 ± 0.39	0.21
Trabecular bone			
DB2	60033.17 ± 7152.34	59126.4 ± 6381.39	0.77
BV/TVB2	0.67 ± 0.17	0.71 ± 0.19	0.53
BS/BVB2	3.47 ± 2.05	2.75 ± 2.04	0.31
TBTHB2	0.91 ± 0.55	1.16 ± 0.91	0.21
TBNB2	0.97 ± 0.31	0.77 ± 0.38	0.37
TBSPB2	0.33 ± 0.11	0.33 ± 0.13	0.99

D, density; BS/BV, bone surface to bone volume; BV/TV, bone volume to tissue volume; TBN, trabecular number; TBSP, trabecular spacing; and TBTH, trabecular thickness. B1 denotes extracranial, B2 middle, and B3 endocranial surfaces. ***p<0.05**.

5.5.1. Sex differences in HFI and control group

When comparing micro-architectural parameters between males with HFI and without HFI across the infraorbital foramen, a significant difference in bone mineral density was observed in both extracranial and endocranial regions of the cortical region (P = 0.03; P = 0.02). Males with HFI had a significantly higher bone mineral density, indicating denser cortical bone in this region compared to males without HFI. Similarly, males with HFI had significantly higher bone mineral density than those without HFI in the trabecular region (P = 0.05). Males with HFI had a decreased bone-volume-to-tissue-volume ratio (BV/TV) in both the cortical and trabecular region compared to males without, with a significant difference observed only in the endocranial surface of the

cortical bone (P = 0.05). Males with HFI had an increased bone-surface-to-bone-volume ratio (BS/BV) in both the cortical and trabecular regions compared to males without HFI. No significant differences were observed between the two groups, indicating similar bone surface area relative to bone volume in this region (Table 6). A decreased trabecular thickness (TBTH) in the trabecular bone was noted in males with HFI compared to those without HFI; however, this difference was not statistically significant (Table 6). Males with HFI had an increased trabecular number (TBN) and trabecular spacing (TBSP) in the trabecular bone compared to those without HFI; however, the differences were not statistically significant (Table 6).

Table 6. Micro-architectural parameters in males with and without HFI (SD - standard deviation) across the infraorbital foramen region.

Micro-architectural parameter	Males with HFI *N* = 8 (Mean ± SD)	Males without HFI *N* = 7 (Mean ± SD)	*P*-value
Cortical bone			
DA1	63327.44 ± 4321.51	57190.79 ± 4045.67	**0.03***
DA3	63780.88 ± 3313.72	56637.14 ± 5687.57	**0.02***
BV/TVA1	0.74 ± 0.19	0.84 ± 0.16	0.65
BV/TVA3	0.52 ± 0.12	0.68 ± 0.20	**0.05***
BS/BVA1	0.59 ± 0.39	0.56 ± 0.51	0.20
BS/BVA3	1.39 ± 0.48	1.02 ± 0.46	0.17
Trabecular bone			
DA2	60822.5 ± 6353.3	54581.07 ± 5248.79	**0.05***
BV/TVA2	0.65 ± 0.32	0.74 ± 0.22	0.17
BS/BVA2	3.92 ± 3.4	2.49 ± 2.56	0.32
TBTHA2	1.06 ± 1.21	13.00 ± 30.95	0.42
TBNA2	0.61 ± 0.42	0.59 ± 0.38	0.51
TBSPA2	0.52 ± 0.37	0.39 ± 0.16	0.12

D, density; BS/BV, bone surface to bone volume; BV/TV, bone volume to tissue volume; TBN, trabecular number; TBSP, trabecular spacing; and TBTH, trabecular thickness. B1 denotes extracranial, B2 middle, and B3 endocranial surfaces. ***p<0.05**.

When comparing micro-architectural parameters in the cortical region across the lateral nasal aperture, males with HFI exhibited higher bone mineral density in both the extra and endocranial surfaces than males without HFI (Table 7). However, a significant difference was only observed in the endocranial surface of the cortical bone ($P = 0.02$; Table 7). Bone mineral density in the trabecular region was significantly higher in males with HFI than those without ($P = 0.02$). Males with HFI had a decreased bone-volume-to-tissue-volume ratio (BV/TV) in both the cortical and trabecular regions, compared to males without HFI. However, the differences between the two groups were not statistically significant (Table 7). Males with HFI had an increased bone-surface-to-bone-volume ratio (BS/BV) in both the cortical and trabecular regions, compared to males without HFI and no significant difference was observed (Table 7).

In the trabecular region, males with HFI had a decreased trabecular thickness (TBTH) and trabecular number (TBN) compared to males without HFI; however, the differences between the two groups were not statistically significant (Table 6). In contrast, males with HFI had an increased trabecular spacing (TBSP) in the trabecular region compared to males without HFI, with no significant difference observed between the two groups (Table 7).

Table 7. Micro-architectural parameters in males with and without HFI (SD - standard deviation) across the lateral nasal aperture region.

Micro-architectural parameter	Males with HFI *N* = 8 (Mean ± SD)	Males without HFI *N* = 7 (Mean ± SD)	*P*-value
Cortical bone			
DB1	63792.06 ± 2501.06	57209.00 ± 4286.52	0.93
DB3	63279.19 ± 4300.64	56703.86 ± 4342.70	**0.02***
BV/TVB1	0.63 ± 0.2	0.73 ± 0.17	0.25
BV/TVB3	0.52 ± 0.18	0.57 ± 0.22	0.77
BS/BVB1	0.95 ± 0.5	0.65 ± 0.40	0.76
BS/BVB3	1.13 ± 0.3	1.06 ± 0.37	0.62
Trabecular bone			
DB2	62141.31 ± 5507.86	54358.14 ± 5033.82	**0.02***
BV/TVB2	0.68 ± 0.17	0.75 ± 0.18	0.97
BS/BVB2	3.15 ± 2.07	2.29 ± 1.86	0.30
TBTHB2	0.95 ± 0.47	9.50 ± 21.97	0.17
TBNB2	0.91 ± 0.33	9.15 ± 22.12	0.73
TBSPB2	0.35 ± 0.11	0.30 ± 0.16	0.50

D, density; BS/BV, bone surface to bone volume; BV/TV, bone volume to tissue volume; TBN, trabecular number; TBSP, trabecular spacing; and TBTH, trabecular thickness. B1 denotes extracranial, B2 middle, and B3 endocranial surfaces. ***p<0.05**.

When comparing micro-architectural parameters across the infraorbital foramen, it was found that females with HFI had a decreased bone mineral density than those without HFI in both the cortical and trabecular regions (Table 8). However, a significant difference was only observed on the endocranial surface of the cortical region (Table 8). Additionally, females with HFI exhibited a decreased bone-volume-to-tissue-volume ratio (BV/TV) at the extracranial surface of the cortical region compared to females without HFI. Nonetheless, this difference was not statistically significant (Table 8). Conversely, an increased bone-volume-to-tissue-volume ratio (BV/TV) was observed in females with HFI at the endocranial surface of the cortical region and in the trabecular region. However, these differences were not statistically significant either (Table 8). Furthermore,

females with HFI had an increased bone-surface-to-bone-volume ratio (BS/BV) at the extracranial surface of the cortical region and in the trabecular region compared to females without HFI. However, these differences were not statistically significant (Table 8). In contrast, females with HFI had a decreased bone-surface-to-bone-volume ratio (BS/BV) at the endocranial surface of the cortical region compared to females without HFI, with no significant difference observed (Table 8). In the trabecular region, females with HFI showed a decreased trabecular thickness (TBTH) and trabecular number (TBN), as well as increased trabecular spacing (TBSP) compared to females without HFI, but these differences were not statistically significant (Table 8).

Table 8. Micro-architectural parameters in females with and without HFI (SD - standard deviation) across the infraorbital foramen region.

Micro-architectural parameter	Females with HFI *N* = 7 (Mean ± SD)	Females without HFI *N* = 8 (Mean ± SD)	*P*-value
Cortical bone			
DA1	61616.57 ± 4197.02	64314.50 ± 2966.28	0.10
DA3	59953.86 ± 6401.61	64105.94 ± 2481.95	**<.001***
BV/TVA1	0.75 ± 0.21	0.77 ± 0.25	0.64
BV/TVA3	0.51 ± 0.16	0.47 ± 0.19	0.78
BS/BVA1	0.67 ± 0.5	0.65 ± 0.40	0.91
BS/BVA3	1.64 ± 0.74	1.80 ± 1.50	0.56
Trabecular bone			
DA2	58934.14 ± 6342.09	64273.69 ± 2637.05	0.07
BV/TVA2	0.73 ± 0.23	0.72 ±0 .15	0.56
BS/BVA2	3.18 ± 2.24	2.53 ± 1.39	0.50
TBTHA2	0.67 ± 0.55	1.89 ± 1.60	0.06
TBNA2	0.6 ± 0.37	0.73 ± 0.25	0.52
TBSPA2	0.34 ± 0.3	0.33 ± 0.10	0.11

D, density; BS/BV, bone surface to bone volume; BV/TV, bone volume to tissue volume; TBN, trabecular number; TBSP, trabecular spacing; and TBTH, trabecular thickness. B1 denotes extracranial, B2 middle, and B3 endocranial surfaces. ***p<0.05**.

When comparing micro-architectural parameters across the lateral nasal aperture, females with HFI had a decreased bone mineral density and bone-volume-to-tissue-volume ratio (BV/TV) in

both the cortical and trabecular regions compared to females without HFI; however, significant differences were only noted on the endocranial surface of the cortical region for both parameters (Table 9). Additionally, females with HFI showed an increased bone-surface-to-bone-volume ratio (BS/BV) in both the cortical and trabecular regions compared to those without HFI. However, these differences were not statistically significant (Table 9). In the trabecular region, females with HFI had decreased trabecular thickness (TBTH) and trabecular spacing (TBSP) and an increased trabecular number (TBN) compared to those without HFI, none of which were statistically significant (Table 9). None of the observed differences in both males and females across the infraorbital foramen and lateral nasal aperture regions were statistically significant following the Bonferroni correction (adjusted P = 0.0021).

Table 9. Micro-architectural parameters in females with and without HFI (SD - standard deviation) across the lateral nasal aperture region.

Micro-architectural parameter	Females with HFI *N* = 7 (Mean ± SD)	Females without HFI *N* = 8 (Mean ± SD)	*P*-value
Cortical bone			
DB1	62210.71 ± 3699.33	64354.50 ± 3338.96	0.07
DB3	61236.57 ± 4045.72	64362.50 ± 2558.35	**0.06***
BV/TVB1	0.59 ± 0.2	0.76 ± 0.24	0.70
BV/TVB3	0.55 ± 0.16	0.67 ± 0.20	**0.43***
BS/BVB1	0.83 ± 0.29	0.65 ± 0.55	0.24
BS/BVB3	1.38 ± 0.64	1.01 ± 0.43	0.18
Trabecular bone			
DB2	57623.86 ± 8442.36	63298.63 ± 4134.51	0.11
BV/TVB2	0.66 ± 0.18	0.67 ± 0.20	0.74
BS/BVB2	3.84 ± 2.11	3.16 ± 2.24	0.78
TBTHB2	0.87 ± 0.66	1.27 ± 1.05	0.11
TBNB2	1.04 ± 0.29	0.85 ± 0.38	0.22
TBSPB2	0.32 ± 0.12	0.36 ± 0.12	0.91

D, density; BS/BV, bone surface to bone volume; BV/TV, bone volume to tissue volume; TBN, trabecular number; TBSP, trabecular spacing; and TBTH, trabecular thickness. B1 denotes extracranial, B2 middle, and B3 endocranial surfaces. ***p<0.05**.

5.5.2. Population differences in HFI and control groups

When comparing micro-architectural parameters between various population groups across the infraorbital foramen, all population groups with HFI presented with an increased bone mineral density compared to those without HFI in both trabecular and cortical regions (Table 10). The SA Black sample with HFI had a decreased bone-volume-to-tissue-volume ratio (BV/TV) compared to those without in both the cortical and trabecular regions (Table 10). In contrast, the SA White sample with HFI had an increased bone-volume-to-tissue-volume ratio (BV/TV) compared to those without in both the cortical and trabecular regions (Table 10). Meanwhile, the SA Coloured sample with HFI had a decreased bone-volume-to-tissue-volume ratio (BV/TV) compared to those without in the cortical region and an increase in the trabecular region (Table 10). In the cortical region, the SA Black sample had an increased bone-surface-to-bone-volume ratio (BS/BV) at the extracranial surface and a decrease at the endocranial surface compared to those without HFI (Table 10). Conversely, in the cortical region, the SA White sample had a decreased bone-surface-to-bone-volume ratio (BS/BV) at the extracranial surface and an increase at the endocranial surface compared to those without HFI (Table 10). In the SA Coloured sample, an increased bone-surface-to-bone-volume ratio (BS/BV) was observed at both the extracranial and endocranial surfaces, compared to those without HFI (Table 10). In the trabecular region, all population groups with HFI presented with an increased bone-surface-to-bone-volume ratio (BS/BV) compared to those without HFI (Table 10).

When comparing trabecular bone-related micro-architectural parameters, the SA Black population with HFI had a decreased trabecular thickness (TBTH) and an increased trabecular number (TBN) and trabecular spacing (TBSP), compared to those without (Table 10). In SA White and SA Coloured populations with HFI, individuals had a decreased trabecular thickness (TBTH), trabecular number (TBN) and trabecular spacing (TBSP), compared to those without (Table 10).

Table 10. Micro-architectural parameters differences in populations with and without HFI (SD - standard deviation) across the infraorbital foramen region.

Microarchitectural Parameter	SA Black with HFI *N* = 4 (Mean ± SD)	SA Black without HFI *N* = 6 Mean ± SD)	SA White with HFI *N* = 6 (Mean ± SD)	SA White without HFI *N* = 7 (Mean ± SD)	SA Coloured with HFI *N* = 5 (Mean ± SD)	SA Coloured without HFI *N* = 2 (Mean ± SD)
Cortical Region						
DA1	63601.00 ± 2938.17	59000.92 ± 5351.31	64177.67 ± 2755.03	62525.86 ± 4723.58	59693.10 ± 5531.25	61582.50 ± 5589.68
DA3	63088.50 ± 3933.33	58149.17 ± 6446.01	63246.58 ± 5225.20	62348.21 ± 5021.04	59618.10 ± 6165.84	61987.50 ± 5016.92
BV/TV A1	0.64 ± 0.05	0.90 ± 0.09	0.77 ± 0.24	0.68 ± 0.25	0.81 ± 0.19	0.96 ± 0.05
BV/TV A3	0.48 ± 0.09	0.58 ± 0.26	0.55 ± 0.14	0.54 ± 0.21	0.50 ± 0.17	0.63 ± 0.27
BS/BVA1	0.73 ± 0.20	0.45 ± 0.37	0.57 ± 0.52	0.86 ± 0.42	0.62 ± 0.50	0.19 ± 0.19
BS/BVA3	1.06 ± 0.26	1.76 ± 1.77	1.62 ± 0.63	1.22 ± 0.61	1.73 ± 0.67	1.22 ± 0.49
Trabecular Region						
DA2	59396.00 ± 5113.57	56647.17 ± 7716.67	62045.25 ± 6321.29	62532.86 ± 4422.87	57852.70 ± 7235.27	59322.00 ± 6104.45
BV/TV A2	0.61 ± 0.30	0.75 ± 0.22	0.75 ± 0.25	0.73 ± 0.18	0.67 ± 0.32	0.64 ± 0.02
BS/BVA2	4.05 ± 3.64	2.42 ± 2.67	2.50 ± 2.38	2.45 ± 1.66	3.06 ± 3.11	2.99 ± 0.12
TBTHA2	0.87 ± 0.55	1.92 ± 1.94	0.86 ± 1.40	13.25 ± 30.84	3.22 ± 6.22	0.94 ± 0.36
TBNA2	0.78 ± 0.15	0.57 ± 0.31	0.60 ± 0.42	0.69 ± 0.35	0.47 ± 0.47	0.88 ± 0.09
TBSPA2	0.52 ± 0.43	0.33 ± 0.17	0.27 ± 0.29	0.37 ± 0.11	0.40 ± 0.34	0.44 ± 0.10

D, density; BS/BV, bone surface to bone volume; BV/TV, bone volume to tissue volume; TBN, trabecular number; TBSP, trabecular spacing; and TBTH, trabecular thickness. B1 denotes extracranial, B2 middle, and B3 endocranial surfaces.

When comparing micro-architectural parameters across the lateral nasal aperture among different population groups, the following trends were observed.

The SA Black sample with HFI had increased bone mineral density in both cortical and trabecular regions, with higher bone-volume-to-tissue-volume (BV/TV) and bone-surface-to-bone-volume ratios (BS/BV) in the cortical region compared to those without HFI (Table 11). However, the trabecular region's bone-surface-to-bone-volume ratio (BS/BV) was lower. In the trabecular region, trabecular thickness (TBTH) and trabecular spacing (TBSP) were decreased, while the trabecular number (TBN) remained similar to those without HFI (Table 11).

The SA White sample with HFI had increased bone mineral density in the cortical region but decreased bone mineral density in the trabecular region compared to those without HFI (Table 11). The bone-volume-to-tissue-volume ratio (BV/TV) increased in the cortical region and decreased in the trabecular region, while the bone-surface-to-bone-volume ratio (BS/BV) was higher in both regions (Table 10). In the trabecular region, trabecular thickness (TBTH), trabecular number (TBN), and trabecular spacing (TBSP) were all reduced compared to those without HFI (Table 11).

The SA Coloured sample with HFI had a decreased bone mineral density in the cortical region and increased bone mineral density in the trabecular region (Table 11). The bone-volume-to-tissue-volume ratio (BV/TV) increased in the cortical region but decreased in the trabecular region. However, the bone-surface-to-bone-volume ratio (BS/BV) was higher in both regions (Table 11). In the trabecular region, trabecular thickness (TBTH) and trabecular number (TBN) were reduced, while trabecular spacing (TBSP) increased compared to those without HFI (Table 11).

Table 11. Micro-architectural parameters differences in populations with and without HFI (SD - standard deviation) across the lateral nasal aperture region.

Microarchitectural Parameter	SA Black with HFI *N* = 4 (Mean ± SD)	SA Black without HFI *N* = 6 Mean ± SD)	SA White with HFI *N* = 6 (Mean ± SD)	SA White without HFI *N* = 7 (Mean ± SD)	SA Coloured with HFI *N* = 5 (Mean ± SD)	SA Coloured without HFI *N* = 2 (Mean ± SD)
Cortical Region						
DB1	64465.50 ± 1657.50	59231.08 ± 5115.99	63520.67 ± 2680.56	62205.50 ± 5690.36	61365.10 ± 4108.72	62237.00 ± 4664.08
DB3	62481.38 ± 3619.37	59176.08 ± 5145.65	64132.25 ± 3182.06	62075.07 ± 5465.20	60034.10 ± 5181.44	61122.50 ± 6240.22
BV/TV B1	0.70 ± 0.19	0.77 ± 0.16	0.56 ± 0.25	0.70 ± 0.25	0.59 ± 0.12	0.83 ± 0.20
BV/TV B3	0.58 ± 0.14	0.63 ± 0.21	0.59 ± 0.21	0.63 ± 0.25	0.44 ± 0.10	0.58 ± 0.07
BS/BVB1	0.71 ± 0.37	0.60 ± 0.32	0.91 ± 0.54	0.80 ± 0.59	0.82 ± 0.28	0.29 ± 0.18
BS/BVB3	1.10 ± 0.26	0.98 ± 0.38	1.27 ± 0.62	1.07 ± 0.47	1.33 ± 0.51	1.08 ± 0.22
Trabecular Region						
DB2	62560.25 ± 2542.52	57324.33 ± 7321.96	60554.17 ± 8957.48	61274.79 ± 5326.91	57386.30 ± 7638.81	57013.25 ± 8430.48
BV/TV B2	0.75 ± 0.17	0.73 ± 0.14	0.70 ± 0.16	0.71 ± 0.23	0.57 ± 0.17	0.66 ± 0.27
BS/BVB2	2.33 ± 1.48	2.49 ± 1.71	3.38 ± 2.06	2.84 ± 2.50	4.50 ± 2.26	3.22 ± 2.37
TBTHB2	1.33 ± 0.71	1.52 ± 0.99	0.78 ± 0.39	9.40 ± 22.02	0.74 ± 0.50	0.88 ± 0.66
TBNB2	0.76 ± 0.28	0.76 ± 0.35	1.05 ± 0.31	9.21 ± 22.09	1.04 ± 0.30	0.90 ± 0.35
TBSPB2	0.31 ± 0.12	0.35 ± 0.07	0.29 ± 0.10	0.32 ± 0.18	0.41 ± 0.11	0.34 ± 0.17

D, density; BS/BV, bone surface to bone volume; BV/TV, bone volume to tissue volume; TBN, trabecular number; TBSP, trabecular spacing and TBTH, trabecular thickness. B1 denotes extracranial, B2 middle, and B3 endocranial surfaces.

5.5.3. Age correlation

5.5.3.1. Infraorbital foramen region

In the assessment of bone mineral density, the cortical region at the extracranial surface and the trabecular region showed a weak positive correlation with age in both HFI and the control group (Table 12), suggesting that as age increases, bone mineral density increases in these regions for both individuals with HFI and the control group. In contrast, at the endocranial surface, there was a weak negative correlation with age in the HFI group, while a weak positive correlation was noted in the control group (Table 12). This indicates that bone mineral density in this region decreases in individuals with HFI as they age while it increases with age in the control group.

When evaluating the bone-volume-to-tissue-volume ratio (BV/TV) in the HFI group, the extracranial surface at the cortical region exhibited a moderate positive correlation with age, while the control group showed a moderate negative correlation (Table 12). The endocranial surface of the cortical region in the HFI group showed a weak positive correlation with age, whereas the control group showed a weak negative correlation (Table 12). The trabecular region showed weak positive correlations with age in both control and HFI groups (Table 12).

Upon evaluating the bone-surface-to-bone-volume ratio (BS/BV), the cortical region at the extracranial surface exhibited a weak negative correlation with age in the HFI group. In contrast, this region's control group exhibited a weak positive correlation (Table 12). In the HFI group, it was observed that the cortical region at the endocranial surface showed a weak positive correlation with age, while the control group showed a weak negative correlation (Table 12). The trabecular region showed a weak negative correlation between age in HFI and control groups (Table 12).

In examining the micro-architectural of the trabecular region, trabecular thickness (TBTH) showed a weak positive correlation with age in the HFI and control groups (Table 12). Trabecular number (TBN) in both HFI and control groups showed a weak negative correlation with age (Table 12). Trabecular spacing (TBSP) exhibited a notable weak negative correlation with age in the HFI group, while the control group showed a weak positive correlation with age (Table 12).

Table 12. Overview of the correlation coefficients (r) between micro-architectural parameters and age across the infraorbital foramen region in HFI and control groups.

Micro-architectural parameter	Individuals with HFI (r) *N* = 15	Individuals without HFI (r) *N* = 15
Cortical bone		
DA1	0.08	0.13
DA3	- 0.13	0.05
BV/TVA1	0.50	- 0.42
BV/TVA3	0.09	- 0.07
BS/BVA1	- 0.36	0.22
BS/BVA3	0.34	-0 .22
Trabecular bone		
DA2	0.08	0.36
BV/TVA2	0.28	0.02
BS/BVA2	- 0.25	- 0.12
TBTHA2	0.18	0.24
TBNA2	- 0.12	- 0.03
TBSPA2	- 0.28	0.11

D, density; BS/BV, bone surface to bone volume; BV/TV, bone volume to tissue volume; TBN, trabecular number; TBSP, trabecular spacing and TBTH, trabecular thickness. B1 denotes extracranial, B2 middle, and B3 endocranial surfaces.

5.5.3.2. Lateral nasal aperture region

In assessing the bone mineral density, the extracranial surface of the cortical and trabecular regions exhibited weak negative correlations with age in the HFI group and weak positive correlations with age in the control group (Table 13). In contrast, the endocranial surface of the cortical region demonstrated weak positive correlations with age in the HFI and control groups (Table 13).

Upon examining the bone-volume-to-tissue ratio (BV/TV) in the HFI group, the cortical region at the extracranial surface showed a weak positive correlation with age (Table 13). Conversely, the control group demonstrated a moderate positive correlation with age in the HFI group (Table 13). The endocranial surface of the cortical region showed a weak positive correlation with age, while

the control group exhibited a moderate negative correlation with age (Table 13). The trabecular region showed weak positive correlations with age in HFI and control groups (Table 13).

In analysing the bone-surface-to-bone-volume ratio (BS/BV), the extracranial surface of the cortical region showed a weak negative correlation with age in the HFI group, while the control group exhibited a weak positive correlation (Table 13). The endocranial surfaces of the cortical region exhibited a weak positive correlation with age in HFI and control groups (Table 13). The trabecular region showed a weak negative correlation with age in HFI and control groups (Table 13).

When investigating the micro-architectural of the trabecular region, trabecular thickness (TBTH) in the HFI group showed a weak negative correlation with age (Table 13). In contrast, the trabecular thickness (TBTH) in the control group exhibited a positive correlation with age (Table 13), whereas the trabecular number (TBN) demonstrated a weak positive correlation with age in both HFI and control groups (Table 13). Trabecular spacing (TBSP) exhibited a weak negative correlation with age in HFI and control groups (Table 13).

Table 13. Overview of the correlation coefficients (r) between micro-architectural parameters and age across the lateral nasal aperture in HFI and control groups.

Micro-architectural parameter	Individuals with HFI (r) *N* = 15	Individuals without HFI (r) *N* = 15
Cortical bone		
DB1	- 0.27	0.06
DB3	0.11	0.16
BV/TVB1	0.04	- 0.42
BV/TVB3	0.24	- 0.44
BS/BVB1	- 0.03	0.25
BS/BVB3	0.19	0.17
Trabecular bone		
DB2	- 0.14	0.26
BV/TVB2	0.10	0.37
BS/BVB2	- 0.08	- 0.38
TBTHB2	- 0.22	0.24
TBNB2	0.07	0.21
TBSPB2	- 0.09	- 0.20

D, density; BS/BV, bone surface to bone volume; BV/TV, bone volume to tissue volume; TBN, trabecular number; TBSP, trabecular spacing and TBTH, trabecular thickness. B1 denotes extracranial, B2 middle, and B3 endocranial surfaces.

5.6. Severity of HFI

The frontal bone's micro-architecture differed amongst various HFI types within the examined sample (Fig. 12). Across the infraorbital foramen, individuals presenting with HFI Type D exhibited an increased bone mineral density, followed by those with Type B in most cases, with Type C and Type A generally having a decreased bone mineral density (BMD) in both cortical and trabecular regions (Table 14). Individuals presenting with Type D had the highest bone-volume-to-tissue-volume ratio (BV/TV) in all regions except the extracranial surface of the cortical region, whereas Type A had the highest bone-volume-to-tissue-volume ratio (BV/TV) (Table 14). Individuals presenting with Type C exhibited the highest bone-surface-to-bone-volume

ratio (BS/BV) in the extracranial of the cortical region and trabecular region; however, in the endocranial surface of the cortical bone, Type A individuals had a higher bone-surface-to-bone-volume ratio (BS/BV) (Table 14). These differences were not statistically significant ($P \geq 0.05$).

In the trabecular region, individuals presenting with Type A had an increased trabecular thickness (TBTH), followed by Type D, B and C (Table 14). Individuals presenting with Type D had an increased trabecular number (TBN) in the trabecular bone, followed by Type C, B and A (Table 14). Individuals presenting with Type C exhibited an increased trabecular spacing (TBSP), followed by Type B and A, while Type D had the least spacing (Table 14). No significant differences were statistically observed in the trabecular region ($P \geq 0.05$).

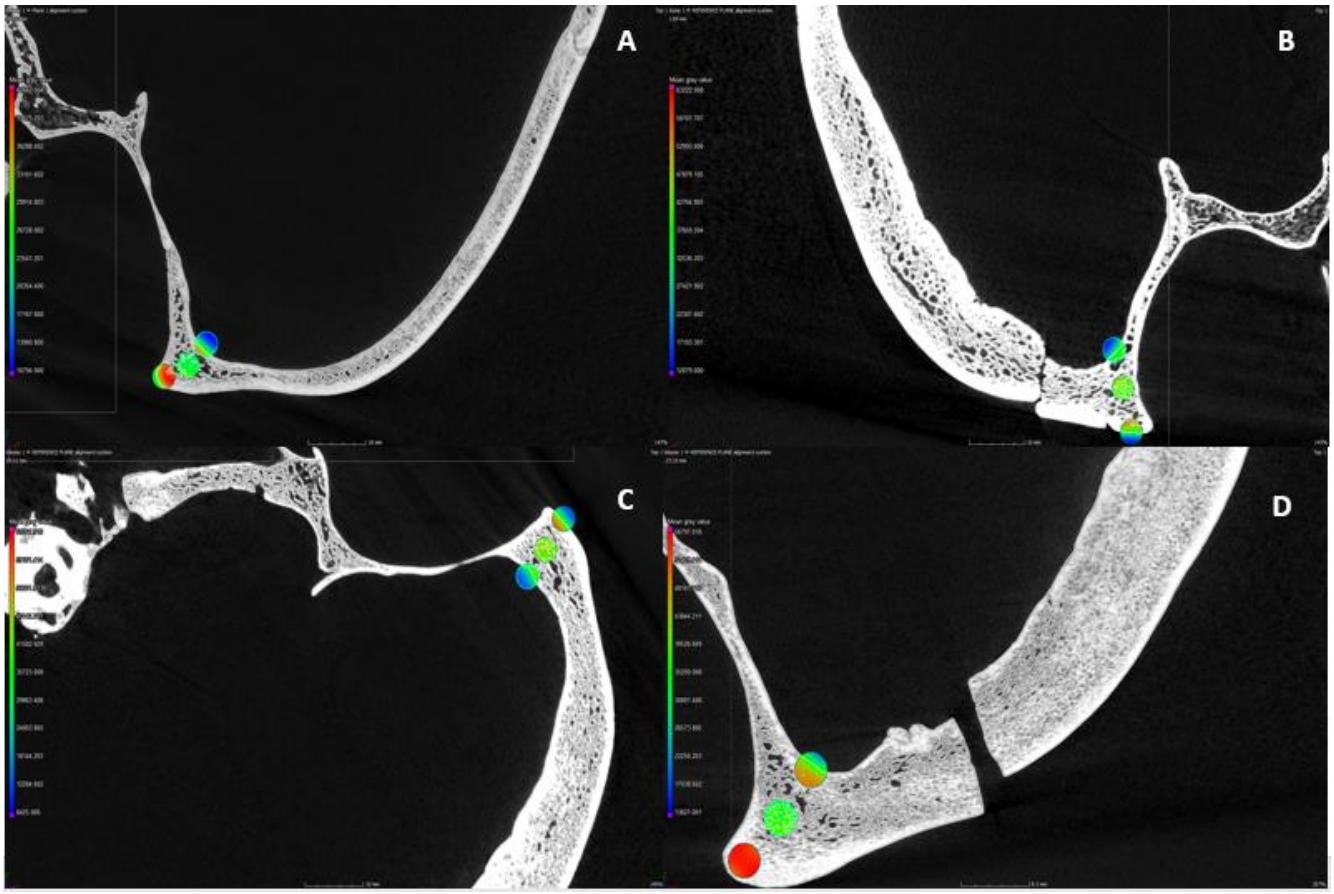


Figure 12. Micro-CT images of individuals presenting HFI Type A (**A**), B (**B**), C (**C**) and D (**D**) through the cranium at the infraorbital foramen region. The colour-coded line reflects variations in density levels. In this gradient, red signifies the highest density, followed by yellow, green, and blue, representing the lowest density.

Table 14. Micro-architectural parameters of cortical and trabecular bone for various HFI types (SD - standard deviation) across the infraorbital foramen region.

Micro-architectural parameter	Type A *N* = 5 (Mean ± SD)	Type B *N* = 4 (Mean ± SD)	Type C *N* = 3 (Mean ± SD)	Type D *N* = 3 (Mean ± SD)
Cortical bone				
DA1	60742.60 ± 4623.55	63813.38 ± 3443.25	61717.00 ± 6612.97	64606.00 ± 815.95
DA3	59126.70 ± 6250.33	62301.38 ± 6467.25	63605.67 ± 3341.70	64756.00 ± 770.64
BV/TVA1	0.88 ± 0.13	0.66 ± 0.20	0.57 ± 0.12	0.82 ± 0.16
BV/TVA3	0.51 ± 0.16	0.46 ± 0.09	0.48 ± 0.08	0.64 ± 0.14
BS/BVA1	0.41 ± 0.35	0.91 ± 0.40	0.94 ± 0.35	0.30 ± 0.30
BS/BVA3	1.70 ± 0.55	1.48 ± 0.46	1.41 ± 0.71	1.31 ± 1.00
Trabecular bone				
DA2	59283.60 ± 5824.97	61071.38 ± 7824.25	56387.00 ± 8163.90	63084.83 ± 2202.74
BV/TV A2	0.78 ± 0.31	0.58 ± 0.21	0.50 ± 0.33	0.86 ± 0.12
BS/BV A2	2.51 ± 3.19	3.89 ± 1.86	5.42 ± 3.82	2.32 ± 1.42
TBTH A2	4.81 ± 6.51	0.57 ± 0.39	0.31 ± 0.11	1.12 ± 0.62
TBNA A2	0.50 ± 0.39	0.70 ± 0.25	0.85 ± 0.23	0.87 ± 0.43
TBSP A2	0.42 ± 0.33	0.45 ± 0.28	0.59 ± 0.53	0.23 ± 0.02

D, density; BS/BV, bone surface to bone volume; BV/TV, bone volume to tissue volume; TBN, trabecular number; TBSP, trabecular spacing and TBTH, trabecular thickness. B1 denotes extracranial, B2 middle, and B3 endocranial surfaces.

In the lateral nasal aperture, individuals presenting with Type D had increased bone mineral density (BMD) in both the cortical and trabecular regions, followed by Type B, C and Type A (Table 15). Individuals with Type A showed the highest bone-volume-to-tissue-volume ratio (BV/TV) in the extracranial surface of the cortical region, followed by Type D and A, while Type C had the lowest compared to other types (Table 15). Bone-volume-to-tissue-volume ratio (BV/TV) values in the endocranial surface of the region were generally similar across types, with Type C slightly higher (Table 15). In the trabecular region, individuals with Type D had an increased bone-volume-to-tissue-volume ratio (BV/TV), followed by Type C, B, and Type A (Table 15). Individuals presenting with Type C had an increased bone-surface-to-bone-volume ratio (BS/BV) across the cortical and trabecular regions (Table 15). Individuals presenting with Type A had a decreased bone-surface-to-bone-volume ratio (BS/BV) in the extracranial surface of the cortical region, while Type D had the lowest in the endocranial surface of the cortical and trabecular regions (Table 15). These differences were not statistically significant ($P \geq 0.05$).

Individuals presenting with Type D had an increased trabecular thickness (TBTH) in the trabecular region, while those with Type C had the lowest trabecular thickness (TBTH) (Table 15). Conversely, individuals with Type C had an increased trabecular number (TBN), with Type D being the lowest (Table 15). Individuals presenting with Type A had an increased trabecular spacing (TBSP), while those with Type D had the lowest trabecular spacing (TBSP) (Table 15). No significant differences were statistically observed in the trabecular region ($P \geq 0.05$).

Table 15. Micro-architectural parameters of cortical and trabecular bone for various HFI types (SD - standard deviation) across the lateral nasal aperture region.

Micro-architectural parameter	Type A *N* = 5 (Mean ± SD)	Type B *N* = 4 (Mean ± SD)	Type C *N* = 3 (Mean ± SD)	Type D *N* = 3 (Mean ± SD)
Cortical bone				
DB1	60346.20 ± 3492.34	64359.25 ± 2351.50	64060.17 ± 2554.49	64821.00 ± 681.28
DB3	60800.40 ± 4400.61	63564.13 ± 3941.75	61888.67 ± 6315.63	63655.00 ± 2807.34
BV/TV B1	0.72 ± 0.17	0.59 ± 0.15	0.42 ± 0.10	0.63 ± 0.27
BV/TV B3	0.52 ± 0.19	0.50 ± 0.21	0.56 ± 0.18	0.57 ± 0.14
BS/BV B1	0.67 ± 0.47	0.88 ± 0.23	0.99 ± 0.09	0.86 ± 0.70
BS/BV B3	1.30 ± 0.58	1.21 ± 0.34	1.44 ± 0.75	1.00 ± 0.27
Trabecular bone				
DB2	59271.80 ± 5965.81	59183.00 ± 11185.82	59515.83 ± 8832.51	62953.00 ± 2264.71
BV/TV B2	0.63 ± 0.21	0.67 ± 0.19	0.59 ± 0.10	0.81 ± 0.07
BS/BV B2	3.74 ± 2.73	3.72 ± 2.44	4.03 ± 0.75	2.14 ± 1.21
TBTHB2	0.95 ± 0.57	0.88 ± 0.48	0.52 ± 0.12	1.30 ± 0.81
TBNB2	0.89 ± 0.34	1.03 ± 0.32	1.16 ± 0.09	0.84 ± 0.41
TBSPB2	0.40 ± 0.12	0.30 ± 0.09	0.37 ± 0.10	0.23 ± 0.04

D, density; BS/BV, bone surface to bone volume; BV/TV, bone volume to tissue volume; TBN, trabecular number; TBSP, trabecular spacing and TBTH, trabecular thickness. B1 denotes extracranial, B2 middle, and B3 endocranial surfaces.

6. DISCUSSION

Understanding the expression of HFI is important, given its increased prevalence in modern populations (Rühli *et al.*, 2004). Despite its occurrence in various global populations, the phenomenon has not been well documented in South African modern skeletal sample, particularly its morphological variation across different demographic groups. This gap in the literature is significant, as ambiguity still surrounds the cause, progression, and clinical significance of HFI (Devriendt *et al.*, 2005). By examining the microarchitectural changes associated with HFI, the biological mechanisms driving excessive bone deposition in the frontal bone can be better understood. For these reasons, the primary aim of this study was to assess the prevalence, expression, and severity of HFI in a South African skeletal sample using a morphological approach. Additionally, this research sought to gain insight into the aetiology and pathogenesis of HFI by examining the micro-architectural changes in affected cranial areas.

The scoring criteria for HFI introduced by Hershkovitz *et al.* (1999) were developed as part of an anthropological study aimed at standardising the classification of this condition across different populations. The criteria proposed by Hershkovitz *et al.* (1999) categorise HFI based on the morphological presentation and severity of bony outgrowths on the internal surface of the frontal bone. The current study effectively used the scoring criteria to identify HFI macroscopically. However, some amendments accounted for variations not noted by Hershkovitz *et al.* (1999). The original scoring criteria lacked the flexibility to include severe cases, such as Type D. In some Type D cases, osseous thickening extended beyond the frontal bone to include the parietal and temporal bones of the endocranial surfaces. These cases were not included in the original scoring criteria but were classified as Hyperostosis cranii interna (HCI) (Hershkovitz *et al.*, 1999). In this study, cases where bony outgrowths extended slightly to adjacent regions, such as the parietal and temporal bones, were classified as Type D. This adaptation aligns with observations by Djonic *et al.* (2016), who noted that while HFI predominantly affects the frontal bone, it can sometimes extend to other cranial regions. When these extensions are more pronounced, they are often classified as HCI, reflecting the broader distribution of the thickening across multiple cranial bones. This finding emphasises the importance of consistent terminology, as Hershkovitz *et al.* (1999) suggested. While HFI is specific to the frontal bone, overlapping or extended cases might

require additional descriptors to clarify the extent of involvement. For instance, "HFI with parietal involvement" could be used to describe such cases while acknowledging their primary origin.

The revised scoring criteria were implemented and subsequently evaluated for intra- and inter-observer reliability. The intra-observer reliability demonstrated a strong level of agreement, with a weighted Cohen's kappa value of $k = 0.891$ ($P < .001$), indicating a high degree of consistency when the primary researcher rescored the expression of HFI. The inter-observer reliability showed a moderate level of agreement, with a weighted Cohen's kappa value of $k = 0.713$ ($P < .001$), suggesting that while there is a reasonable level of consistency between different observers, some variability remains. These findings suggest that the scoring criteria are reliable, but further standardization, such as refining the scoring criteria, may be needed to improve consistency between different observers. The reliability results of this study fall within the range observed in similar studies, as May *et al.* (2010) reported intra- and inter-observer Kappa values of 0.75 and 0.793, respectively, when using a comparable four scale scoring criteria by Hershkovitz *et al*. (1999) to score HFI.

In this study, the overall rate of HFI occurrence was 17.15% in the assessed crania ($n = 2186$). Although the individuals assessed may not proportionally reflect the broader South African population, this prevalence provides valuable insights into the occurrence of HFI in a modern human population in South Africa, contributing to the broader understanding of its distribution across different demographic contexts. To date, this study reports the highest frequency of HFI in modern skeletal populations compared to previous findings, with earlier studies documenting incidences of 12.8% in European and African American samples between the ages of 20 and 80+ years (Hershkovitz *et al*., 1999), 0.8% in individuals of unspecified population affinity from France, aged 42 to 79 years (Devriendt *et al*., 2005), 3.68% in Serbian sample ranging in age from 10 to 101 years (Nikolic *et al*., 2010) and 11.9% in European ethnic group from central and southern Europe region aged 20-94 years (Raikos *et al*., 2011).

In this study, females (64.8%) exhibited a significantly higher prevalence of HFI compared to males (35.2%) despite males comprising 71% of the total sample assessed in the Raymond Dart Collection, indicating a notable sex-related difference in the prevalence of HFI. Comparable rates of HFI occurrence between the sexes have been documented using Hershkovitz *et al.* (1999) scoring criteria, with approximately 20% in females and 3% in males among 404 individuals

assessed (Cvetković *et al.*, 2019). Hershkovitz *et al.* (1999) also documented HFI in 23.9% of females and 5.2% of males within a sample of 1,706 modern skeletal remains. Similarly, Nikolic *et al.* (2010) identified HFI in 18.14% of females and 0.07% of males (only a single case) from a sample of 1,468 crania, while Raikos *et al.* (2011) reported a prevalence of 11.07% in females and 1.23 % in males among 244 examined specimens.

The differences in HFI occurrence between the sexes indicate that sex may play a role in the prevalence or expression of HFI, suggesting a potential biological or hormonal influence, particularly oestrogen and testosterone, on bone mineral density (Riggs *et al*., 2002). In females, oestrogen is crucial for regulating bone metabolism by preserving bone mass and suppressing bone turnover while ensuring a balance between bone formation and resorption rates. It regulates the functional activity of both osteoclasts and osteoblasts by reducing osteoclast formation and activity through increased apoptosis while enhancing osteoblast formation and activity by reducing apoptosis (Chow *et al*., 1992; Manolagas, 2000; Riggs *et al*., 2002). Modern females are exposed to prolonged oestrogen due to fewer pregnancies, reduced breastfeeding periods and widespread use of hormonal contraceptives and hormone replacement therapy (Hershkovitz *et al.*, 1999). The prolonged oestrogen exposure causes a reduced bone turnover and bone remodelling imbalance (suppressing the resorption phase and prolonging the formation phase), leading to the thickening of the frontal bone's inner table (Khosla *et al*., 2012). Thus, an increase or a prolonged oestrogen stimulation in females contribute to irregular bone deposition, such as that seen in HFI (May *et al*., 2011).

In males, testosterone primarily functions in bone metabolism by reducing bone resorption and prolonging the lifespan of osteoblasts and osteoclasts, which ultimately enhances bone formation (Riggs *et al.*, 2002). Much of testosterone's effect on bone occurs through its conversion to oestrogen via aromatization (Western & Bekvalac, 2016). Testosterone increases the periosteal apposition of bone. As a result, males generally develop thicker and denser bones, making them less susceptible to the irregular endocranial thickening characteristic of HFI (May *et al*., 2011). When HFI is present in males, it is generally linked to testicular atrophy and lower androgen levels (Raikos *et al.*, 2011).

This study revealed differences in the prevalence of HFI types between sexes. Type A HFI was found to be slightly more prevalent in males than in females. Conversely, types B, C, and D were

predominantly observed in females. However, the differences observed were not statistically significant (X= 0.904; p = 1.000). While these observations suggest a potential sex-related patterns in HFI progression, the lack of statistical significance indicates that the distribution of HFI types is not influenced by sex. Similarly, Hershkovitz *et al.* (1999) assessed a modern and historical skeletal population along with a smaller cadaver population. In the male skeletal samples, only one case of type C HFI was reported, with no cases of type D (Hershkovitz *et al.*, 1999). Within their cadaver population, the majority of males with HFI exhibited type A, with only one individual presenting type D HFI. Hershkovitz *et al.* (1999) findings were in accordance with the trends observed in Cvetković *et al.* (2019), where males predominantly exhibited milder forms of HFI, with only three males in presenting with type D HFI, suggesting that while rare, type D HFI in males is not entirely absent. The variation in the severity of HFI expression may represent differential susceptibility to the causative factors such as hormonal imbalance (Hershkovitz *et al.*, 1999).

In this study, South African Black individuals exhibited a higher frequency of HFI compared to South African White and Coloured individuals, with significant differences observed between the Black and White populations (p = 0.013). The prevalence amongst the population sample may be attributed to the uneven distribution of populations in the Raymond A. Dart Collection of Modern Human Skeletons, with SA Black individuals comprising 72.78% of the study sample and SA White individuals representing 22.42% (Table 1) (Dayal *et al.*, 2016). Notably, no cases of HFI were identified in the South African Indian sample. The absence of HFI observed in the South African Indian sample was likely due to the limited sample size (n = 4). The distribution of HFI types varied significantly across the population groups. Types A, B, and C were more commonly observed in South African Black individuals, whereas Type D, the most advanced stage, was more prevalent among South African White individuals. This could be due to the variability in the age profiles across the study population groups, potentially leading to bias regarding the observed occurrence of types of HFI. The study sample comprised of more older SA White individuals compared to SA Black and SA Coloured samples (Table 1). The finding that advanced HFI (Type D) is more prevalent in South African White individuals challenges prior assumptions about the uniformity of HFI progression across populations (Hershkovitz *et al.*,1999). This underscores the importance of considering population diversity in studies of cranial bone pathology, specifically HFI.

HFI prevalence was generally higher in individuals aged 50–69 years (38.13%), followed by those aged 70+ years (34.13%) and 20–49 years (27.73%), with no significant age-cohort differences (p = 0.059). Types A, B, and C were more common in middle-aged groups, while Type D was prevalent in older individuals. The distribution of HFI types by age, with more severe forms (Type D) in older individuals, suggests a potential progression of HFI severity with age. However, the correlation between age and severity of HFI was weak (r = 0.150), indicating that the relationship is not strongly supported. Females showed an increase in HFI frequency with age and remained relatively stable between middle and older ages: 20-49 years (n = 64/243; 26.33%), 50-69 years (n = 90/243, 37.03%) and 70+ years (n= 89/243; 36.6%), while males exhibited a decline after middle age: 20-49 (n = 40/132, 30.30%), 50-59 (n = 53/132, 40.15%) and 70+ years (n = 39/132, 29.55%). The age distribution of the assessed sample and life expectancy influenced the observed HFI patterns across age groups. Males in the assessed sample were over-represented in younger (n = 819) and middle-aged (n = 653) groups but notably fewer in the older age group (n = 280). The decline in the older male sample corresponds with the decrease in HFI prevalence, indicating that lower male survival rates may have influenced the results. Fewer older males may have led to an under-representation of severe HFI cases, as individuals with more advanced HFI may not have lived long enough to be included in the study (Dayal *et al.*, 2016).

In contrast, females were fewer overall but more evenly distributed across age groups (n = 321, 226, and 157, respectively). A weak positive correlation was observed in both males (r = 0.122) and females (r = 0.152) when age and the degree of HFI were considered. Given that HFI is known to progress with age (Hershkovitz *et al.*,1999), having a sufficient number of older females ensured a more accurate representation of older cases. The trends observed in this study support Hershkovitz *et al.* (1999) findings, indicating that the relationship between age and HFI prevalence is more evident in females than in males. Additionally, Western and Bekvalac (2016) investigated the relationship between age and the prevalence of HFI in historic female skeletal populations. Comparable to the findings in this study, HFI prevalence in females plateaued from the age of 50-59 years onwards (Western & Bekvalac, 2016). However, Western and Bekvalac (2016) observed a strong positive correlation between age and HFI, with most cases occurring in older females, particularly post-menopausal individuals. Western and Bekvalac (2016) highlighted age and longevity as primary factors in HFI occurrence rather than parity or reproductive patterns.

The SA White sample showed increased HFI prevalence with age, i.e., young age (n = 5/146, 3.42%), middle age (n = 43/146, 29.45%) and old age (n = 98/146, 67.12%), whereas SA Coloured sample displayed a decrease, i.e., young age (n = 12/20, 60%), middle age (n = 5/20, 25%) and old age (n = 3/20, 15%). In the SA Black sample, the frequency of HFI increased from young-aged (n = 87/209, 41.62%) to middle-aged (n = 95/209, 45.45%) and then decreased during older-aged (n = 27/209, 12.92%) individuals. The observed differences in HFI prevalence across the South African population samples may be influenced by variations in age distribution and life expectancy. In SA White individuals, the increase in HFI with age suggests that a greater proportion of individuals living into old age allows for a more accurate representation of HFI's progression. The decrease in HFI prevalence with age in the SA Coloured sample was most probably due to the small sample size, whereas the decrease in HFI prevalence with age among the older SA Black sample may be influenced by social disparities (Dayal *et al.*, 2016) that contribute to lower life expectancy, resulting in an under-representation of HFI severe cases. The correlation between age and HFI severity in both population groups and sex was generally weak, suggesting that while age contributes to the manifestation of HFI, it is not the sole determining factor. Other environmental factors, such as lifestyle and hormonal changes, may play a role in its development (Rühli *et al.,* 2007).

Given the South Africa's diverse population and political history, ethnic disparities persist in various aspects of daily life, influencing socioeconomic conditions, access to resources and lifestyle-related diseases (Micklesfield e*t al.,* 2011). The South African White population typically exhibits greater dietary diversity, incorporating a balanced intake of cereals, meats, dairy products, and a wider variety of fruits and vegetables compared to SA Black and SA Coloured populations (Labadarios *et al*, 2011). Since phytoestrogens are primarily found in fruits and vegetables, their diet may naturally contain higher levels of this compound (Cassidy & Faughnan, 2000). Although a phytoestrogen-rich diet offers health benefits, excessive consumption may induce oestrogenic effects that contribute to the development of HFI (Cassidy & Faughnan, 2000).

Since HFI primarily affects the frontal region, this study investigated its aetiology and pathogenesis by analysing micro-architectural changes in the affected cranial areas. The micro-architectural measurements in this study generally showed a poor agreement in both the inter- and intra- observer repeatability (Table 3). The repeatability results indicated that the measurements in

this study may lack reliability or consistency, highlighting the need for improved measurement methods and enhanced observer training for future research.

To highlight the impact of HFI on frontal bone micro-architecture, a comparison was made between individuals with and without HFI. Increased bone mineral density (BMD) and bone-surface-bone-volume ratio (BS/BV) were observed in individuals with HFI in both cortical and trabecular regions. Due to the small sample size, the differences were not statistically significant. According to Wolff's law, the microarchitecture of the bone is shaped by mechanical stress (Mellon & Tanner, 2012), therefore, the mentioned micro-architectural changes suggest increased bone remodelling activity in individuals with HFI, possibly indicating a compensatory response to the thickened frontal bone. In accordance with our results, Inal *et al*. (2024) investigated the bone thickness and density in individuals with diffuse HFI (a type of HFI where the thickening of the frontal bone is widespread or evenly distributed across the entire frontal region) using cranial computed tomography (CT) scans. The study included 154 adult patients with diffuse HFI and 151 adult patients without HFI as controls (Inal *et al*., 2024). Measurements were taken at the vertex, frontal tuberosity, and frontal sinus levels in the midline, right, and left lateral parts (Inal *et al*., 2024). The findings revealed that bone thickness values were significantly increased at all measured levels in patients with HFI compared to the control group (Inal *et al*., 2024). Additionally, bone densities in the HFI regions were higher at the vertex and frontal tuberosity levels (Inal *et al*., 2024). A positive correlation was observed between bone thickness and density; however, as bone thickness increased, density values decreased (Inal *et al*., 2024). Unfortunately, no studies have simultaneously examined bone mineral density (BMD) and bone-surface-to-bone-volume ratio (BS/BV) in both the cortical and trabecular regions of individuals with HFI as have been done in the current study.

Trabecular bone, also known as cancellous or spongy bone, is a highly porous and metabolically active bone tissue found at the ends of long bones and within flat bones, including the diploë of the skull (Keaveny *et al*., 2001). It is characterised by a network of interconnected trabeculae (thin bony struts or plates) that provide structural support while minimising weight (Keaveny *et al*., 2001). The trabecular skull bone is not uniform in its structure, and its histological characteristics (such as trabecular arrangement, density, and porosity) play a crucial role in determining its mechanical properties (Boruah *et al.*, 2015). It is known that the mechanical properties of the

trabecular bone depend on the proportion of bone tissue relative to the total volume (Keaveny *et al*., 2001). This study found notable differences in trabecular parameters between individuals with and without HFI, specifically, decreased trabecular thickness (TBTH) in both regions and increased trabecular spacing (TBSP) in the infraorbital foramen region. Increased trabecular spacing (TBSP) and decreased trabecular thickness (TBTH) in individuals with HFI suggest significant alterations in bone microarchitecture. The increased trabecular spacing (TBSP) indicates reduced connectivity between trabeculae, leading to wider gaps between bone struts. Although trabecular number (TBN) may be increased, the trabeculae are not as tightly woven, potentially compromising bone strength. Simultaneously, the decrease in trabecular thickness (TBTH) reflects thinner trabeculae, which may result from increased bone resorption or disrupted bone formation. This thinning can weaken the bone, making it more susceptible to fractures or structural instability. These changes likely stem from altered bone remodelling processes influenced by hormonal imbalances or mechanical loading shifts associated with HFI (Adanty *et.al*., 2021).

Sexes were analysed independently to examine variations in micro-architectural parameters in individuals with and without HFI. In this study, males with HFI showed significant alterations in their cranial bone micro-architecture compared to males without HFI, particularly in bone mineral density (BMD). Males with HFI exhibited significantly higher bone mineral density in both the cortical and trabecular regions at the infraorbital foramen and lateral nasal aperture (Tables 6 & 7). This increased density, particularly in the endocranial surfaces, suggests a pattern of excessive bone deposition and mineralisation. These findings are consistent with the hyperostotic nature of HFI, where abnormal bone growth is concentrated in specific cranial regions i.e., the frontal bone (Hershkovitz *et al.* 1999). The higher BMD in these regions reflects the characteristic bone remodelling associated with HFI and is likely a key factor in its higher prevalence among individuals with this condition (Rühli *et al.,* 2007).

In addition to the increased BMD, males with HFI displayed a significant decrease in the bone-volume-to-tissue-volume ratio, particularly in the endocranial cortical bone at the infraorbital foramen. This decrease indicates that while bone density may be higher, the overall quality of the bone is compromised. This finding suggests that the bone in individuals with HFI may be more densely packed but structurally weaker, most likely resulting from abnormal growth patterns

associated with this condition. Excessive osteoblastic activity leads to increased bone mineral density (BMD), resulting in thicker and denser bone (Rowe *et al*., 2023). However, if remodelling is disorganised, trabecular connectivity may be impaired, weakening the overall bone structure (Rowe *et al*., 2023). Additionally, insufficient osteoclastic resorption can cause the accumulation of old or poor-quality bone, making it brittle and more prone to fractures (Rowe *et al*., 2023). This imbalance in bone turnover may contribute to the altered microarchitecture observed in individuals with HFI. The decrease in this ratio is significant because it points to potential disruptions in the normal bone remodelling process, which may explain the prevalence of HFI in individuals with altered bone turnover.

Another key finding in this study was the increase in the bone-surface-to-bone-volume ratio (BS/BV) in males with HFI, observed in both cortical and trabecular regions. Although this difference was not statistically significant (Tables 6 & 7), the increase suggests an abnormal remodelling pattern with irregular or excessive bone surface development. This could indicate a hyperplastic response in the bone tissue, contributing to the distinctive bony projections seen in HFI. Despite the absence of statistical significance, this trend further highlights the complex nature of bone remodelling in HFI and its potential impact on cranial morphology, which may help explain the observed prevalence of the condition in different sexes.

Regarding trabecular micro-architecture, males with HFI demonstrated decreased trabecular thickness and increased trabecular spacing in the trabecular bone compared to those without HFI. However, the differences observed were not statistically significant (Tables 6 & 7). The decreased trabecular thickness could reflect localised disruptions in bone quality, while the increased trabecular spacing might indicate a less dense, more porous trabecular network in certain areas (Adanty *et.al*., 2021). These changes suggest that although HFI is characterised by increased bone density overall, there may be regions where the trabecular structure is weakened, which could contribute to a paradoxical decrease in mechanical strength despite denser bone (Adanty *et.al*., 2021).

Although an increase in bone mass is expected to correspond with a higher trabecular number (Goulet *et al.,* 1994), the observed variations in trabecular number showed no significant differences due to the small sample size. These micro-architectural changes in trabecular structure may further contribute to the heterogeneous presentation of HFI, suggesting that the condition

manifests differently across individuals, potentially explaining the variability in its clinical and radiographic features.

In contrast to males' results, females with HFI exhibited decreased bone mineral density (BMD) in both the cortical and trabecular regions and decreased trabecular number (TBN) compared to females without HFI. The decrease in bone mineral density (BMD) and trabecular number (TBN) suggests bone loss, i.e., osteoporosis. Osteoporosis is a chronic pathological condition characterized by decreased bone mineral density (BMD), leading to a reduction in bone strength and an increased susceptibility to fractures. (Pothiwala *et al.,* 2006). It is prevalent in postmenopausal females (Guggenbuhl, 2009), largely due to oestrogen deficiency, which is a significant factor in its development (Raisz, 2005). When oestrogen levels decline, it results to decreased bone formation and increased bone resorption, ultimately contributing to osteoporosis (Raisz, 2005). Oestrogen deficiency stimulates osteoclast activity, enhancing bone resorption while impairing osteoblast function, which reduces bone formation (Raisz, 2005). This disruption of the balance between bone resorption and formation results in a net loss of bone mass (Raisz, 2005). Consequently, the absence of oestrogen leads to an imbalance in bone remodelling, which is a primary driver of osteoporosis, particularly in postmenopausal females (Raisz, 2005).

Conversely, a study by Bracanovic *et al.* (2016) reported different trends in bone micro-architecture associated with HFI. Bracanovic *et al.* (2016) analysed 1×1 cm samples from the thickest part of the frontal bone in 20 women with HFI (age: 69.9 ± 11.1 years) and 14 women without HFI (age: 74.1 ± 9.7 years) using micro-CT. Bracanovic *et al.* (2016) assessed the 3D bone microarchitecture across four regions of interest: total sample, outer table, diploe and inner table. The study revealed that women with HFI exhibited a significantly increased bone volume fraction in the diploic region, characterized by thicker and more plate-like trabeculae, along with reduced trabecular separation and connectivity density (Bracanovic *et al.*, 2016). Additionally, the inner table of the frontal bone in the HFI group showed significantly higher total porosity and mean pore diameter compared to controls (Bracanovic *et al.*, 2016). The microstructural reorganisation was further evidenced by a notably higher porosity and lower bone volume fraction in the inner table relative to the outer table, attributed to an increased trabecular number (Bracanovic *et al.*, 2016).

The findings of Bracanovic *et al.* (2016) supported the Global Model of HFI pathogenesis proposed by Hershkovitz *et al*. (1999), highlighting the role of hormonal and metabolic changes,

especially in postmenopausal women. The study highlights that oestrogen deficiency, a key factor in menopause, may drive excessive osteoblastic activity, leading to increased bone volume fraction (BV/TV), thicker and more plate-like trabeculae, and reduced trabecular separation in individuals with HFI (Bracanovic *et al.*, 2016). Additionally, the significantly higher porosity observed in the inner table, along with the presence of large pores (>100 μm), suggests an imbalance in bone remodelling, where excessive bone formation is accompanied by localized bone resorption (Bracanovic *et al.*, 2016). The microarchitectural changes observed in this study align with the Global Model's premise that HFI develops through a disrupted interplay of bone formation and resorption rather than a uniform thickening process (Bracanovic *et al.*, 2016).

The microarchitectural findings in the cortical region, characterized by increased bone mineral density (BMD) and bone surface-to-bone volume ratio (BS/BV) alongside decreased bone volume-to-total volume ratio (BV/TV), align with the process of diploization as described by the global model of Hyperostosis frontalis interna (HFI) pathogenesis. The observed reduction in bone-volume-to-tissue-volume (BV/TV) suggests a loss of compact cortical bone mass, while the elevated bone surface-to-bone volume ratio (BS/BV) indicates increased surface irregularity, likely resulting from the formation of new vascular channels and active bone remodeling at resorption deposition interfaces (Hershkovitz *et al*., 1999). Despite the decreased cortical volume fraction, the increased bone mineral density (BMD) reflects the presence of highly mineralized lamellar bone, consistent with ongoing osteogenic activity.

In the trabecular region, the observed decrease in trabecular thickness (TBTH), combined with increases in trabecular number (TBN) and trabecular separation (TBSP), further supports the global model's prediction of irregular neo-osteogenesis and remodeling within the diploë (Hershkovitz *et al*., 1999). This pattern reflects both enhanced bone formation and architectural disorganization. These changes result from dural vascular ingrowth that stimulates osteogenesis, driving the progressive thickening of the inner cortical layer toward the endocranial cavity, as described by the global model (Hershkovitz *et al*., 1999). However, the global model does not fully explain all aspects of the present findings. The concurrent increase in trabecular number (TBN) and separation (TBSP) suggests that remodelling within the diploë may involve both the formation of new trabecular struts and localized resorption events that create greater inter-trabecular spacing (Adanty *et.al*., 2021).

Across both the infraorbital foramen and lateral nasal aperture, individuals with HFI exhibited increased bone mineral density (BMD) in cortical and/or trabecular regions, with variations in bone-volume-to-tissue-volume (BV/TV) and bone-surface-to-bone-volume (BS/BV) ratios that differed among population groups. At the infraorbital foramen, all groups with HFI showed increased BMD in both cortical and trabecular regions, a consistent feature of the condition. However, bone-volume-to-tissue-volume (BV/TV) decreased in the cortical regions of SA Black and Coloured samples but increased in both cortical and trabecular regions of SA White sample. Similarly, bone-surface-to-bone-volume (BS/BV) in the cortical region followed unique patterns: the SA Black sample exhibited an extracranial increase and endocranial decrease, the SA White sample showed the reverse trend, and the SA Coloured sample had an increase at both surfaces. Across the lateral nasal aperture, population-specific trends emerged. For instance, the SA Black sample had increased bone mineral density and bone-volume-to-tissue-volume (BV/TV) in cortical bone. In contrast, the SA White sample demonstrated increased cortical bone mineral density (BMD) but decreased trabecular bone mineral density (BMD), and the SA Coloured sample showed the opposite trend to the SA White sample.

Regarding the trabecular micro-architecture, the SA Black sample at both anatomical regions maintained higher trabecular number (TBN) and trabecular spacing (TBSP) but reduced trabecular thickness (TBTH), reflecting a robust but less dense trabecular network. By contrast, the SA White and Coloured sample consistently exhibited decreased trabecular thickness (TBTH), trabecular number (TBN), and trabecular spacing (TBSP) at the infraorbital foramen. At the same time, SA Coloured individuals showed increased trabecular spacing (TBSP) alongside reduced trabecular thickness (TBTH) and trabecular number (TBN) at the lateral nasal aperture.

The findings reveal distinct population-specific adaptations to HFI, underscoring how bone micro-architecture responds to the condition's metabolic and structural demands. The consistent increase in bone mineral density (BMD) across most groups suggests that HFI universally stimulates greater mineralisation, potentially as a compensatory mechanism for maintaining structural stability. However, the variation in bone-volume-to-tissue-volume (BV/TV) and bone-surface-to-bone-volume (BS/BV) ratios across regions and groups reflects differing strategies for balancing bone density, volume, and surface complexity (Burr, 2019). For example, the reduced cortical BV/TV in SA Black and Coloured samples may indicate less bone volume relative to tissue volume,

potentially offset by changes in trabecular number and spacing to preserve mechanical strength (Burr, 2019). Meanwhile, SA White samples increased in cortical bone-volume-to-tissue-volume ratio (BV/TV) could signify a denser, more compact cortical structure (Burr, 2019).

Trabecular changes observed highlight further complexity. SA Black sample's higher trabecular number (TBN) and trabecular spacing (TBSP), alongside reduced trabecular thickness (TBTH), suggest a well-distributed but thinner trabecular network, which may enhance load distribution despite reduced bone mineral density (Seeman & Delmas, 2006). Conversely, the consistently reduced trabecular parameters (thickness, number, spacing) in SA White and Coloured samples point to weaker trabecular networks, especially in areas of decreased bone mineral density, raising concerns about potential fragility. This may have occurred due to osteoporosis, as individuals of European descent are more susceptible to the condition (Pothiwala *et al.*, 2006). The anatomical regions also show site-specific responses. Differences between the infraorbital foramen and lateral nasal aperture highlight how local biomechanical demands or vascular factors might shape bone remodelling. For instance, the SA Coloured population's increased trabecular spacing at the lateral nasal aperture may reflect compensatory adaptations to differing functional stresses compared to the infraorbital foramen.

The analysis in the current study highlights differential age-related patterns in bone micro-architecture between individuals with HFI and controls, reflecting bone mineral density (BMD), volume, and structure variations. In the cortical region at the extracranial surface, bone mineral density (BMD) showed a weak positive correlation with age in the HFI group, contrasting with a weak negative correlation in the control sample. The slight increase in bone mineral density (BMD) with age may be due to a compensatory increase in bone density caused by abnormal bone deposition resulting from HFI (Rowe *et al*., 2023). In this study, the age distribution of the control sample ranged from 40 to 77 years, a period in which both cortical and trabecular bone strength naturally decline by approximately 2–5% and 5–10%, respectively (Burr, 2019). Therefore, the decrease in bone mineral density (BMD) in the control group is likely because, in healthy individuals, aging typically causes bone resorption to outpace bone formation, especially in the cortical bone, leading to a decline in bone mineral density (BMD) (Burr, 2019). At the endocranial surface, the correlation pattern was reversed, showing a weak negative correlation in the HFI group and a weak positive correlation in the control group. The weak negative correlation in the HFI

group is possibly due to increased porosity in the endocranial surface of the cortical bone. According to Bracanovic *et al.* (2016), as HFI develops, larger pores occur as a result of penetration of blood vessels from the dura, ultimately leading to diploization of the inner table, leading to reduced overall bone mineral density (BMD). The bone-volume-to-tissue-volume ratio (BV/TV) followed similar patterns, where the cortical extracranial surface exhibited a moderate positive correlation in the HFI group and a moderate negative correlation in controls (Tables 12 & 13), suggesting that, as age increases, bone-volume-to-tissue-volume ratio (BV/TV) increases in individuals with HFI. Despite the potential for increased porosity and weaker structure in the newly formed bone, the continuous deposition of excessive bone over time leads to an increase in bone volume at the extracranial surface of the cortical region (Burr, 2019). In the control group, aging typically leads to a decrease in bone volume in cortical regions due to the loss of trabecular support and decline in bone mass (Burr, 2019). The bone volume possibly decreased as age increases, due to bone resorption.

Further differences emerged in the bone-surface-to-bone-volume ratio (BS/BV) (Tables 12 & 13). At the extracranial cortical surface, a weak negative correlation was noted in the HFI group, while controls showed a weak positive correlation; in the trabecular region, both groups exhibited weak negative correlations with age. Micro-architectural analysis of trabecular bone revealed that trabecular thickness (TBTH) had a weak negative correlation with age in the HFI group but a weak positive one in controls. Both groups showed weak positive correlations for trabecular number (TBN), yet trabecular spacing (TBSP) differed, with a weak negative correlation in the HFI group and a weak positive correlation in controls. These findings suggest that HFI may influence age-related changes in bone structure, with distinct patterns emerging in cortical and trabecular regions compared to controls. The observed correlations in bone micro-architecture with age are very weak, indicating limited statistical significance. These results are likely influenced by the advanced average age of the SA White sample, which may reduce variability in age-related trends. Moreover, the absence of age stratification in the analysis could obscure more nuanced patterns, as the sample's demographic skew may mask the potential effects of HFI on bone characteristics across different age groups. Future studies should incorporate age-stratified comparisons with a larger sample size to address this limitation.

The micro-architecture of the frontal bone differed across various types of HFI. In most cortical and trabecular regions assessed, Type D had an increased bone mineral density (BMD) followed by Type B, while Types C and A typically had lower densities. Type D also exhibited the highest bone-volume-to-tissue-volume ratio (BV/TV) in most regions except the extracranial cortical surface, where Type A was dominant. For the bone-surface-to-bone-volume ratio (BS/TV), Type C was highest in certain regions. Although trabecular parameters like thickness, number, and spacing showed differences across HFI types, these differences were not statistically significant. The variations in bone micro-architecture among different HFI types suggest that individuals with more severe forms of HFI (such as Type D) tend to exhibit stronger bone mineral density, bone-volume-to-tissue-volume ratio (BV/TV), and trabecular characteristics, especially in the cortical and trabecular regions. However, these differences were not statistically significant due to the small sample size, indicating that while certain trends exist, they may not be conclusive in determining the direct link between HFI severity and bone characteristics. These results imply that bone characteristics could be influenced by HFI type, but more research is needed with a larger sample size to confirm any definitive patterns.

7. CONCLUSION

To date, no research has assessed the prevalence of HFI in South African skeletal samples. This study offers valuable insights into its occurrence within this population, enhancing the understanding of its expression in a South African context. The findings confirm that while HFI is not exclusive to females, its prevalence and severity are significantly higher in females. Among population groups, SA Black individuals exhibited a higher frequency of HFI, whereas severe cases were more commonly observed in SA White individuals. However, due to the limited sample size, particularly among SA Indian and Coloured individuals, these prevalence estimates may not fully represent the broader South African population. Additionally, no clear correlation was found between HFI severity and age. The effective use of Hershkovitz *et al.* (1999) scoring criteria highlights its applicability; however, modifications to the Type D classification are recommended to account for cases where HFI extends beyond the frontal bone. For future research, it would be beneficial to expand the sample size to include a more diverse representation of the South African

population, especially considering different population groups such as South African Indian and Coloured populations. Additionally, stratifying by age, sex, and other demographic factors could provide deeper insights into how these variables may influence the prevalence and expression of HFI.

Based on our results, it can be concluded that microarchitectural structure of the frontal bone varies between individuals with and without HFI, across sex, age, and population groups. These results support the theory that hormonal changes are a critical factor in the development of HFI and align with the "Global Model" proposed by Hershkovitz *et al.* (1999), which attributes HFI to hormonal regulation and metabolic health factors affecting the diploe region of the frontal bone. Although HFI is hypothesized to alter the microarchitectural structure of the frontal bone, health disparities among population groups, such as variations in the prevalence of osteoporosis, also affect the overall bone health of the frontal bone. However, the severity of HFI could not be differentiated at the microstructural level. Importantly, the poor intra-and inter observer repeatability and small sample size limit the conclusiveness of these observations. Although this study provides imperative preliminary evidence for a link between HFI and changes in the microarchitectural structure of the frontal bone, future research involving larger, more demographically representative samples and quantitative observer reliability testing is needed to validate these findings and further investigate the functional implications of HFI-related changes in frontal bone structure.

REFERENCES

Adanty, K., Rabey, K.N., Doschak, M.R., Bhagavathula, K.B., Hogan, J.D., Romanyk, D.L., Adeeb, S., Ouellet, S., Plaisted, T.A., Satapathy, S.S. and Dennison, C.R., 2021. Cortical and trabecular morphometric properties of the human calvarium. *Bone*, *148*, p.115931.

Andersson, A.M. and Skakkebaek, N.E., 1999. Exposure to exogenous estrogens in food: possible impact on human development and health. *European Journal of Endocrinology*, *140*(6), pp.477-485.

Allan, J.C, 1982. Learning about Statistics: A Primer in Simple Statistical Methods for Students of the Medical, Biological, Paramedical, Social and Behavioral Sciences. Johannesburg, RSA: Macmillan South Africa.

Attanasio, F., Granziera, S., Giantin, V. and Manzato, E., 2013. Full penetrance of Morgagni-Stewart-Morel syndrome in a 75-year-old woman: case report and review of the literature. *The Journal of Clinical Endocrinology & Metabolism*, *98*(2), pp. 453-457.

Barber, G., Watt, I. And Rogers, J., 1997. A comparison of radiological and palaeopathological diagnostic criteria for hyperostosis frontalis interna. *International Journal of Osteoarchaeology, 7(2),* pp. 157-164.

Bartelheimer, H., 1939.Hyperostosis Frontalis Interna and Hypophysaren Diabetes. *Deutsche Medizinische Wochenschrift, 65*, pp.1129-1130.

Boruah, S., Paskoff, G.R., Shender, B.S., Subit, D.L., Salzar, R.S. and Crandall, J.R., 2015. Variation of bone layer thicknesses and trabecular volume fraction in the adult male human calvarium. *Bone*, *77*, pp.120-134.

Bracanovic D., Djonic D., Nikolic S., Milovanovic P., Rakocevic Z., Zivkovic V. and Djuric M., 2016. 3D-Microarchitectural patterns of Hyperostosis frontalis interna: a micro-computed tomography study in aged women. *Journal of Anatomy*, 229, pp.673–680.

Bracanovic, D., Djuric, M., Sopta, J., Bracanovic, M. and Djonic, D., 2020. Radiological evaluation of Hyperostosis frontalis interna: is it of clinical importance? *Homo*, *71*(2), pp. 155-160.

Burr, D.B., 2019. Changes in bone matrix properties with aging. *Bone*, *120*, pp.85-93.

Calame, M.A., 1951. Hyperostosis frontalis interna. *Revue Médicale de la Suisse Romande*, *71*(11), pp.748–750.

Callewaert, F., Sinnesael, M., Gielen, E., Boonen, S. and Vanderschueren, D., 2010. Skeletal sexual dimorphism: relative contribution of sex steroids, growth hormone-insulin-like growth factor-I (GH-IGF-I) and mechanical loading. *Journal of Endocrinology*, *207*(2), pp.127-134.

Cassidy, A. and Faughnan, M., 2000. Phyto-oestrogens through the life cycle. *Proceedings of the Nutrition Society*, *59*(3), pp.489-496.

Chen, H., Zhou, X., Fujita, H., Onozuka, M. and Kubo, K.Y., 2013. Age-related changes in trabecular and cortical bone microstructure. *International Journal of Endocrinology*, *2013*(1), p.213234.

Chow, J., Tobias, J.H., Colston, K.W. and Chambers, T.J., 1992. Estrogen maintains trabecular bone volume in rats not only by suppression of bone resorption but also by stimulation of bone formation. *The Journal of Clinical Investigation*, *89*(1), pp.74-78.

Christmas, C., O'Connor, K.G., Harman, S.M., Tobin, J.D., Münzer, T., Bellantoni, M.F., Clair, C.S., Pabst, K.M., Sorkin, J.D. and Blackman, M.R., 2002. Growth hormone and sex steroid effects on bone metabolism and bone mineral density in healthy aged women and men. *The Journals of Gerontology Series A: Biological Sciences and Medical Sciences*, *57*(1), pp.M12-M18.

Cvetković, D., Nikolić, S., Brković, V. and Živković, V., 2020. Hyperostosis frontalis interna as an age-related phenomenon–Differences between males and females and possible use in identification. *Science & Justice*, *59*(2), pp. 172-176.

Dayal, M.R., Kegley, A.D., Štrkalj, G., Bidmos, M.A. and Kuykendall, K.L., 2009. The history and composition of the Raymond A. Dart Collection of human skeletons at the University of the Witwatersrand, Johannesburg, South Africa. *American Journal of Physical Anthropology: The Official Publication of the American Association of Physical Anthropologists*, *140*(2), pp.324-335.

Devriendt, W., Piercecchi-Marti, M.D., Adalian, P., Sanvoisin, A., Dutour, O. and Leonetti, G., 2005. Hyperostosis frontalis interna: forensic issues. *Journal of Forensic Science*, *50*(1), pp. 143-6.

Djonic, D., Bracanovic, D., Rakocevic, Z., Ivovic, M., Nikolic, S., Zivkovic, V. and Djuric, M., 2016. Hyperostosis frontalis interna in postmenopausal women-Possible relation to osteoporosis. *Women & Health*, *56*(8), pp. 994-1007.

Glab, H., Szostek, K. and Kaczanowski, K., 2006. Hyperostosis frontalis interna, a genetic disease?. Two medieval cases from Southern Poland. *Homo-Journal of Comparative Human Biology*. *57*(1), pp.19-27.

Goulet, R., Goldstein, S.A., Ciarelli, M.J., Kuhn, J.L., Brown, M.B. and Feldkamp, L.A., 1994. The relationship between the structural and orthogonal compressive properties of trabecular bone. *Journal of Biomechanics*, *27*(4), pp.375-389.

Guggenbuhl, P., 2009. Osteoporosis in males and females: is there really a difference?. *Joint Bone Spine*, *76*(6), pp.595-601.

Hajdu, T., Fóthi, E., Bernert, Z., Molnár, E., Lovász, G., Ko, I., Köhler, K. and Marcsik, A., 2009. Appearance of hyperostosis frontalis interna in some osteoarcheological series from Hungary. *Homo*, *60*(3), pp.185-205.

Hershkovitz, I., Greenwald, C., Rothschild, B.M., Latimer, B., Dutour, O., Jellema, L.M. and Wish-Baratz, S., 1999. Hyperostosis frontalis interna: an anthropological perspective. *American Journal of Physical Anthropology*, *109*(3), pp. 303-325.

Inal, M., Muluk, N.B. and Celik, E.N., 2024. The multidetector CT evaluation of diffuse hyperostosis frontalis interna. *Romanian Journal of Rhinology*, *14*(55).

Jaffe, H.L., 1972. Metabolic, degenerative, and inflammatory diseases of bones and joints. In *Metabolic, degenerative, and inflammatory diseases of bones and joints* (pp. 10-1101).

Keaveny, T.M., Morgan, E.F., Niebur, G.L. and Yeh, O.C., 2001. Biomechanics of trabecular bone. *Annual Review of Biomedical Engineering*, *3*(1), pp.307-333.

Khosla, S., Oursler, M.J. and Monroe, D.G., 2012. Estrogen and the skeleton. *Trends in Endocrinology & Metabolism*, *23*(11), pp.576-581.

Knies, P.T. and Le Fever, H.E., 1941. Metabolic craniopathy: hyperostosis frontalis interna. *Annals of Internal Medicine*, *14*, pp.1858–1892.

Kramer, B., Hutchinson, E.F., Brits, D.M. and Billings, B.K., 2019. Making the ethical transition in South Africa: Acquiring human bodies for training in anatomy. *Anatomical Sciences Education*, *12*(3), pp.264-271.

Korenman, S., 1980. Oestrogen window hypothesis of the aetiology of breast cancer. *The Lancet*, *315*(8170), pp.700-701.

Labadarios, D., Steyn, N.P. and Nel, J., 2011. How diverse is the diet of adult South Africans?. *Nutrition Journal*, *10*, pp.1-11.

Lahlou, N., Landais, P., De Boissieu, D. and Bougneres, P.F., 1997. Circulating leptin in normal children and during the dynamic phase of juvenile obesity: relation to body fatness, energy metabolism, caloric intake, and sexual dimorphism. *Diabetes*, *46*(6), pp. 989-993.

Manolagas, S.C., 2000. Birth and death of bone cells: basic regulatory mechanisms and implications for the pathogenesis and treatment of osteoporosis. *Endocrine Reviews*, *21*(2), pp.115-137.

Marlet, J.J.C., 1974. Development of cranial hyperostosis. *Radiology Clinical Biology 43*(6), pp. 473–482.

May, H., Peled, N., Dar, G., Hay, O., Abbas, J., Masharawi, Y. and Hershkovitz, I., 2010. Identifying and classifying hyperostosis frontalis interna via computerized tomography. *The Anatomical Record*, *293*(12), pp. 2007-2011.

May, H., Peled, N., Dar, G., Abbas, J. and Hershkovitz, I., 2011a. Hyperostosis frontalis interna: what does it tell us about our health? *American Journal of Human Biology*, *23*(3), pp. 392-397.

May, H., Peled, N., Dar, G., Cohen, H., Abbas, J., Medlej, B. and Hershkovitz, I., 2011b. Hyperostosis frontalis interna: criteria for sexing and aging a skeleton. *International Journal of Legal Medicine*, *125*(5), pp. 669-673.

May, H., Mali, Y., Dar, G., Abbas, J., Hershkovitz, I. and Peled, N., 2012. Intracranial volume, cranial thickness, and hyperostosis frontalis interna in the elderly. *American Journal of Human Biology*, *24*(6), pp.812-819.

McBride, G.B., 2005. A proposal for strength-of-agreement criteria for Lin's concordance correlation coefficient. *NIWA Client Report: HAM2005-062*, *45*, pp.307-310.

McHugh, M.L., 2012. Interrater reliability: the kappa statistic. *Biochemia Medica*, *22*(3), pp.276-282.

McKusick, V.A., 1978. *Mendelian inheritance in man. Baltimore and London*: The Johns Hopkins University Press.

Mellon, S.J. and Tanner, K.E., 2012. Bone and its adaptation to mechanical loading: a review. *International Materials Reviews*, *57*(5), pp.235-255.

Micklesfield, L.K., Norris, S.A. and Pettifor, J.M., 2011. Ethnicity and bone: a South African perspective. *Journal of Bone and Mineral Metabolism*, *29*, pp.257-267.

Moore, S., 1955. Hyperostosis cranii; Stewart-Morel syndrome; metabolic craniopathy; Morgagni's syndrome; Stewart-Morel-Moore syndrome (Ritvo); le syndrome de Morgagni-Morel. Thomas.

Morel, F., 1951. Hyperostosis frontalis interna and cerebral symptoms. *Confinia Neurologica*, *11*(1), pp.9–13.

Morgagni, GB. 1719. *Adversaria anatomica, VI*. *Animadversio LXXIV*. Padua: Vulporius.

Mulhern, D.M., Wilczak, C.A. and Dudar, J.C., 2006. Brief communication: unusual finding at Pueblo Bonito: multiple cases of hyperostosis frontalis interna. *American Journal of Physical Anthropology: The Official Publication of the American Association of Physical Anthropologists*, *130*(4), pp.480-484.

Murphy, E., Kortyna, R. and Flaherty, D., 2018. Hyperostosis Frontalis: A Review. *Journal of Orthopaedics for Physician Assistants*, *6*(2), p.p.17.

Nikolic, S., Djonic, D., Vladimir, Z., Babic, D., Jukovic, F. and Djuric, M., 2010. Rate of occurrence, gross appearance, and age relation of hyperostosis frontalis interna in females: a prospective autopsy study. *The American Journal of Forensic Medicine and Pathology*, *31*(3), pp.205-207.

Perou, M., 1964. *Cranial hyperostosis*. Springfield, IL: Charles C. Thomas.

Pothiwala, P., Evans, E.M. and Chapman-Novakofski, K.M., 2006. Ethnic variation in risk for osteoporosis among women: a review of biological and behavioral factors. *Journal of Women's Health*, *15*(6), pp.709-719.

Raikos, A., Paraskevas, G.K., Yusuf, F., Kordali, P., Meditskou, S., Al-Haj, A. and Brand-Saberi, B., 2011. Etiopathogenesis of hyperostosis frontalis interna: A mystery still. *Annals of Anatomy-Anatomischer Anzeiger*, *193*(5), pp.453-458.

Raisz, L.G., 2005. Pathogenesis of osteoporosis: concepts, conflicts, and prospects. *The Journal of Clinical Investigation*, *115*(12), pp.3318-3325.

Riggs, B.L., Khosla, S. and Melton III, L.J., 2002. Sex steroids and the construction and conservation of the adult skeleton. *Endocrine Reviews*, *23*(3), pp.279-302.

Rosatti, P., 1972. A family affected by hyperostosis frontalis interna (Morgagni-Morel syndrome) across four successive generations. *Journal de Génétique Humaine*, *20*, pp.207–252.

Rowe, P., Koller, A. and Sharma, S., 2018. Physiology, bone remodelling.

Rühli, F.J. and Henneberg, M., 2002. Are hyperostosis frontalis interna and leptin linked? A hypothetical approach about hormonal influence on human microevolution. *Medical Hypotheses*, *58*(5), pp.378-381.

Rühli, F.J., Böni, T. and Henneberg, M., 2004. Hyperostosis frontalis interna: archaeological evidence of possible microevolution of human sex steroids? *Homo*, *55*(1-2), pp.91-99.

Rühli, F.J., Kuhn, G., Evison, R., Müller, R. and Schultz, M., 2007. Diagnostic value of micro-CT in comparison with histology in the qualitative assessment of historical human skull bone pathologies. *American Journal of Physical Anthropology*, *133*(4), pp.1099-1111.

Salmi, A., Voutilainen, A., Holsti, I.R. and Unnerus, C.E., 1962. Hyperostosis cranii in a normal population. *The American Journal of Roentgenology, Radium Therapy, and Nuclear Medicine*, *87*, pp.1032-1040.

Santen, R.J., 1975. Is aromatization of testosterone to estradiol required for inhibition of luteinizing hormone secretion in men?. *The Journal of Clinical Investigation*, *56*(6), pp.1555-1563.

Schober, P., Boer, C., & Schwarte, L. A. 2018. Correlation Coefficients: Appropriate Use and Interpretation. *Anesthesia & Analgesia*, *126*(5), pp.1763-1768.

Seeman, E. and Delmas, P.D., 2006. Bone quality—the material and structural basis of bone strength and fragility. *New England Journal of Medicine*, *354*(21), pp.2250-2261.

She, R. and Szakacs, J., 2004. Hyperostosis frontalis interna: case report and review of literature. *Annals of Clinical & Laboratory Science*,*34*(2), pp.206-208.

Stewart, R., 1928. Localized cranial hyperostosis in the insane. *Journal of Neurology and Psychopathology*, 8, pp.321–331.

Strassmann, B.I., 1999. Menstrual cycling and breast cancer: an evolutionary perspective. *Journal of Women's Health*, *8*(2), pp.193-202.

Szeniczey, T., Marcsik, A., Ács, Z., Balassa, T., Bernert, Z., Bakó, K., Czuppon, T., Endrődi, A., Évinger, S., Farkas, Z. and Hlavenková, L., 2019. Hyperostosis frontalis interna in ancient populations from the Carpathian Basin–A possible relationship between lifestyle and risk of development. *International Journal of Paleopathology*, *24*, pp.108-118.

Thevoz, F., 1966. The dura mater and its vessels in the morphogenesis of hyperostosis frontalis interna. In *Annales d'anatomie Pathologique*, *11*(2), pp.121-149.

Topaloğlu, Ö., Bayraktaroğlu, T., Tekin, S., Topaloğlu, S.N., Şahin, İ. and Cantürk, Z., 2022. Hyperostosis Frontalis Interna. *Turkish Journal of Endocrinology & Metabolism*, *26*(4).

Watrous, A.C., Anton, S.C. and Plourde, A.M., 1993. Hyperostosis frontalis interna in ancient Egyptians. *American Journal of Physical Anthropology*, 16, pp.205.

Western, A.G. and Bekvalac, J.J., 2016. Hyperostosis frontalis interna in female historic skeletal populations: Age, sex hormones and the impact of industrialization. *American Journal of Physical Anthropology*,*162*(3), pp.501-515.

Yamakawa, K., Mizutani, K., Takahashi, M., Matsui, M. and Mezaki, T., 2006. Hyperostosis frontalis interna associated with hypogonadism in an elderly man. *Age and Ageing*, *35*(2), pp.202-203.

Appendix A. Ethics waiver from the Human Ethics Research Committee of the University of the Witwatersrand permitting for the use of skeletal samples from Raymond A. Dart collection.

UNIVERSITY OF THE WITWATERSRAND, JOHANNESBURG

FACULTY OF HEALTH SCIENCES

Anatomical Sciences

SCHOOL OF ANATOMICAL SCIENCES ETHICS WAIVER CLEARANCE LETTER

Faculty of Health Sciences

School of Anatomical Sciences University of the Witwatersrand Johannesburg

Re: In terms of Chapter 8, sections 62-64 of the National Health Act No 61 of 2003 donated bodies and their tissues may be used for, among other purposes, health, and research. Use of such Material is subject only to permission from the responsible person in the School of Anatomical Sciences – the Head or person designated by the Head of School.

Human Research Ethics Committee (Medical) Clearance Certificate:

W-CBP-220504-01

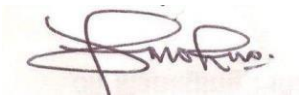
This letter serves to confirm that the Head of School, based in the School of Anatomical Sciences, Faculty of Health Sciences, has reviewed the research proposal entitled:

An assessment of hyperostosis frontalis interna within a South African skeletal sample

by principal investigator: Mmanoko Irene Moraba

and Supervisor/Collaborators: Dr A. Meyer and Prof E.F. Hutchinson

has granted approval for the ethics waiver to conduct the above-mentioned research study.



Professor Amadi O Ihunwo

School of Anatomical Sciences

Faculty of Health Sciences

Appendix B: An assessment of age normality within HFI types using the Shapiro–Wilk Test.[1]

Age	*N*	Shapiro-Wilk W	*P*-value	Normality
25	3	0.75	0	Not normal
28	6	0.496	0	Not normal
32	8	0.809	0.036	Not normal
35	3	0.75	0	Not normal
36	4	0.863	0.272	Normal
38	6	0.831	0.11	Normal
40	11	0.876	0.093	Normal
42	5	0.828	0.135	Normal
43	5	0.552	0	Not normal
45	15	0.771	0.002	Not normal
47	5	0.771	0.046	Not normal
48	5	0.883	0.325	Normal
49	5	0.684	0.006	Not normal
50	15	0.827	0.008	Not normal
52	5	0.821	0.119	Normal
53	5	0.771	0.046	Not normal
54	3	1	1	Normal
55	6	0.775	0.035	Not normal
56	5	0.684	0.006	Not normal
57	5	0.883	0.325	Normal
58	9	0.892	0.208	Normal
59	6	0.823	0.093	Normal
60	24	0.86	0.003	Not normal
61	4	0.729	0.024	Not normal

[1] Normality distribution was not assessed for individuals aged 34,68,94 and 100 due to small sample size (n <3).

62	7	0.769	0.02	Not normal
63	3	0.75	0	Not normal
64	7	0.84	0.099	Normal
65	10	0.878	0.124	Normal
66	5	0.833	0.146	Normal
67	4	0.63	0.001	Not normal
69	15	0.876	0.041	Not normal
70	15	0.649	0	Not normal
71	3	0.75	0	Not normal
72	4	0.849	0.224	Normal
73	6	0.908	0.421	Normal
74	4	0.63	0.001	Not normal
75	11	0.815	0.015	Not normal
76	4	0.895	0.406	Normal
77	4	0.729	0.024	Not normal
78	6	0.64	0.001	Not normal
79	3	1	1	Normal
80	11	0.878	0.097	Normal
81	3	0.75	0	Not normal
82	5	0.803	0.086	Normal
83	5	0.684	0.006	Not normal
84	8	0.843	0.082	Normal
85	8	0.912	0.366	Normal
86	5	0.821	0.119	Normal
88	5	0.902	0.421	Normal
89	4	0.729	0.024	Not normal
90	3	0.75	0	Not normal

Appendix C: An assessment of normality in HFI type distribution among population groups using the Shapiro–Wilk Test.

Population group	*N*	Shapiro-Wilk W	*P*-value	Normality
SA White	146	0.85	< 0.001	Not normal
SA Black	209	0.83	< 0.001	Not normal
SA Coloured	20	0.743	< 0.001	Not normal

Appendix D: An assessment of normality in HFI type distribution among sexes using the Shapiro–Wilk Test.

Sex	*N*	Shapiro-Wilk W	*P*-value	Normality
Male	132	0.753	< 0.001	Not normal
Female	243	0.86	< 0.001	Not normal

Appendix E. Shapiro–wilk test of normality for Micro-CT variables assessed in control (C) and HFI groups.

Variable	Group	*N*	Shapiro-Wilk W	*P*-value	Normality
DA1	C	15	0.877	0.042	Not Normal
	HFI	15	0.87	0.034	Not Normal
DA2	C	15	0.833	0.01	Not Normal
	HFI	15	0.753	<0.001	Not Normal
DA3	C	15	0.826	0.008	Not Normal
	HFI	15	0.754	0.001	Not Normal
DB1	C	15	0.718	<0.001	Not Normal
	HFI	15	0.875	0.04	Not Normal
DB2	C	15	0.926	0.237	Normal
	HFI	15	0.922	0.205	Normal
DB3	C	15	0.842	0.013	Not Normal
	HFI	15	0.867	0.03	Not Normal
BV/TVA1	C	15	0.931	0.284	Normal

	HFI	15	0.96	0.698	Normal
BV/TVA2	C	15	0.948	0.499	Normal
	HFI	15	0.983	0.986	Normal
BV/TVA3	C	15	0.926	0.234	Normal
	HFI	15	0.948	0.491	Normal
BV/TVB1	C	15	0.877	0.043	Not Normal
	HFI	15	0.939	0.369	Normal
BV/TVB2	C	15	0.951	0.545	Normal
	HFI	15	0.951	0.542	Normal
BV/TVB3	C	15	0.976	0.94	Normal
	HFI	15	0.949	0.506	Normal
BS/BVA1	C	15	0.933	0.298	Normal
	HFI	15	0.876	0.041	Not Normal
BS/BVA2	C	15	0.93	0.277	Normal
	HFI	15	0.944	0.437	Normal
BS/BVA3	C	15	0.748	<0.001	Not Normal
	HFI	15	0.84	0.013	Not Normal
BS/BVB1	C	15	0.976	0.934	Normal
	HFI	15	0.825	0.008	Not Normal
BS/BVB2	C	15	0.966	0.794	Normal
	HFI	15	0.896	0.081	Normal
BS/BVB3	C	15	0.976	0.94	Normal
	HFI	15	0.949	0.506	Normal
TBTHA2	C	15	0.344	<0.001	Not Normal
	HFI	15	0.892	0.072	Normal
TBTHB2	C	15	0.32	<0.001	Not Normal
	HFI	15	0.847	0.016	Not Normal
TBNA2	C	15	0.931	0.286	Normal
	HFI	15	0.925	0.232	Normal
TBNB2	C	15	0.294	<0.001	Not Normal

	HFI	15	0.969	0.845	Normal
TBSPA2	C	15	0.928	0.251	Normal
	HFI	15	0.764	0.001	Not Normal
TBSPB2	C	15	0.935	0.318	Normal
	HFI	15	0.949	0.508	Normal

D, density; BS/BV, bone surface to bone volume; BV/TV, bone volume to tissue volume; TBN, trabecular number; TBSP, trabecular spacing; and TBTH, trabecular thickness. Region A, Measurements across the infraorbital region and region B, measurements across the lateral nasal aperture. A1/B1 denotes extracranial, B1/B2 middle, and B3/B3 endocranial surfaces

Appendix F. Distribution of individuals assessed with absence of HFI (*n* = 1811).

Sex	Age cohorts	SA African	SA white	SA coloured	SA Indian
Females	20-29	63	2	3	0
	30-39	74	1	5	0
	40-49	52	5	4	0
	50-59	46	17	4	0
	60-69	30	36	5	0
	70-79	12	31	1	0
	80-89	2	30	1	0
	90+	0	2	0	0
Males	20-29	97	4	3	0
	30-39	214	22	9	0
	40-49	256	33	11	1
	50-59	251	60	12	0
	60-69	186	53	9	2
	70-79	69	43	9	1
	80-89	24	4	7	0

90+	6	4	2	0
Total	**1382**	**344**	**85**	**4**

Appendix G: Distribution of HFI types in females, by age and population groups.

	SA African HFI Type				SA White HFI Type				SA Coloured HFI Type				
Age	A	B	C	D	A	B	C	D	A	B	C	D	**Total**
20-29	7	2	0	1	0	0	0	0	0	1	0	0	**11**
30-39	7	5	3	4	0	0	0	0	1	0	0	0	**20**
40-49	4	12	7	3	1	1	0	0	1	2	1	1	**33**
50-59	8	8	8	4	4	3	0	1	1	1	0	0	**38**
60-69	4	14	6	3	3	11	7	3	0	0	0	1	**52**
70-79	1	9	1	0	5	5	5	10	1	1	0	0	**38**
80-89	3	3	1	1	6	10	8	10	0	0	0	0	**42**
90+	1	2	0	0	2	1	2	1	0	0	0	0	**9**
Total	**35**	**55**	**26**	**16**	**21**	**31**	**22**	**25**	**4**	**5**	**1**	**2**	**43**
Grand Total		**132**				**99**					**12**		

Appendix H: Distribution of HFI types in males, by age and population groups.

	SA African				SA White				SA Coloured				
	HFI Type				HFI Type				HFI Type				
Age	A	B	C	D	A	B	C	D	A	B	C	D	**Total**
20-29	3	1	0	0	0	0	0	0	0	0	0	0	**4**
30-39	7	1	1	0	0	0	0	0	0	0	1	0	**10**
40-49	10	4	3	2	2	0	0	1	4	0	0	0	**26**
50-59	9	4	5	1	1	1	1	0	2	0	0	0	**24**
60-69	12	6	1	2	5	2	0	1	0	0	0	0	**29**
70-79	1	2	0	0	5	7	3	3	1	0	0	0	**22**
80-89	1	0	0	0	4	7	1	0	0	0	0	0	**13**
90+	0	1	0	0	3	0	0	0	0	0	0	0	**4**
Total	**43**	**19**	**10**	**5**	**20**	**17**	**5**	**5**	**7**	**0**	**1**	**0**	**132**
Grand Total		**77**				**47**				**8**			